Advances in Nano Research, *Vol. 12, No. 3 (2022) 301-317*
https://doi.org/10.12989/anr.2022.12.3.301

A biodegradable magnesium alloy sample induced rat osteochondral defect repair through Wnt/β-catenin signaling pathway

Kexin Zhao[1,2,3], Yingqi Chen[2,3], Fei Yu[2,3], Weng Jian[2,3], Ming Zheng[4,5] and Hui Zeng*[2,3]

[1]*Department of Bone & Joint Surgery, Peking University Shenzhen Hospital, Shenzhen Peking University-The Hong Kong University of Science and Technology Medical Center, Guangdong province China*
[2]*Department of Bone & Joint Surgery, Peking University Shenzhen Hospital, Shenzhen, PR China, 518036*
[3]*National & Local Joint Engineering Research Center of Orthopaedic Biomaterials, Peking University Shenzhen Hospital, Shenzhen, PR China, 518036*
[4]*Department of Physiology and Pathophysiology, School of Basic Medical Sciences, Health Science Center, Peking University, Beijing, China,100191*
[5]*Key Laboratory of Molecular Cardiovascular Science, Ministry of Education, Beijing, China*

(*Received December 31, 2020, Revised January 14, 2021, Accepted January 15, 2021*)

Abstract. Many studies have shown that Mg-Nd-Zn-Zr (abbreviated as JDBM) alloy has good biocompatibility and biodegradability as well as promotion of cell adhesion, proliferation and differentiation, and Wnt/β-catenin signaling pathway may play a unique role in joint tissue by controlling the function of chondrocytes, osteoblasts and synoviocytes. However, it is not clear whether the JDBM alloy induces osteochondral repair through Wnt/β-catenin signaling pathway. This study aims to verify that JDBM alloy can repair osteochondral defects in rats, which is realized by Wnt/β-catenin signaling pathway.
In this study, the osteochondral defect model of the right femoral condyle non-weight-bearing area in rats was established and randomly divided into three groups: Control group, JDBM alloy implantation group and JDBM alloy implantation combined with signaling pathway inhibitor drug ICRT3 injection. It was found that after JDBM alloy implantation, the bone volume fraction (BVF) became larger, the bone trabeculae were increased, the relative expression of osteogenesis gene Runx2, Bmp2, Opn, Ocn and chondrogenesis gene Collagen II, Aggrecan were increased, and the tissue repair was obvious by HE and Masson staining, which could be inhibited by ICRT3.
Keywords: biodegradable magnesium alloy; western blot semi-quantitative analysis; Wnt/β-catenin signaling pathway

1. Introduction

Osteochondral defect after trauma or osteoarthritis is a common clinical disease. The thickness of adult osteochondral tissue is about 3-4 mm, including cartilage (90%), calcified cartilage layer (5%) and subchondral bone (5%). From the surface of articular cartilage to subchondral bone, there are chemical composition, mechanical properties and gradient changes in organizational structure. Among them, the cartilage layer of osteochondral structure is complex and has no blood vessels and lymphatic ingrowth, which leads to the lack of self-healing ability of degenerated articular cartilage after injury. Without proper and timely intervention, cartilage defects may penetrate deep into the subchondral bone and arthroplasty surgery is required at the end (Hay *et al*. 2017, Baumann *et al*. 2019). So far, the repair of osteochondral deficiency is still a challenging clinical problem for surgeons (Felson *et al*. 2000, Tounsi *et al*. 2013, Besseghier *et al*. 2015, Bouadi *et al*. 2018, Boutaleb *et al*. 2019, Hussain *et al*. 2019, Kassahun 2019, Mehar and Panda 2019, Semmah *et al*. 2019, Hussain *et al*. 2020, Matouk *et al*. 2020b, Hadji and Avcar 2021).

Currently, clinical treatments have been developed for patients with osteochondral defects, including palliative, restorative and regenerative treatments (Kwon *et al*. 2019). Palliative treatment can relieve knee pain and improve functional status, but it cannot prevent further cartilage defect progression (Kosy *et al*. 2011). Although microfracture technology and other repair methods can fill cartilage defects, the fibrocartilage tissue generated by this repair method lacks the biomechanical and viscoelastic characteristics of natural glassy cartilage (Kreuz *et al*. 2006). Recent osteochondral transplantation with autograft or allograft provides a powerful opportunity to treat severe cartilage defects. Nevertheless, auto transplantation still faces some disadvantages, such as limited donor sources, mismatched mechanical properties and high incidence of donor sites. Disadvantages of allograft include difficulty in graft preservation and management, risk of disease transmission and immunogenicity (Marcacci *et al*. 2013). All these objective reasons lead to the high cost of transplantation and poor transplantation effect, which makes it difficult to carry out effectively in clinic (Islam Molla *et al*. 2018, Huang and Sun 2020, Yan *et al*. 2020, Yang *et al*. 2020, 2021, Hu *et al*. 2021, Li *et al*. 2021, Liu *et al*. 2021c, Lv *et al*. 2021).

In recent years, artificial cartilage scaffold materials for repairing cartilage defects have been widely used in orthopedics, which has attracted much attention because of its good performance (Ming *et al*. 2018). Artificial cartilage

*Corresponding author, Ph.D.,
E-mail: zenghui_36@163.com

ISSN: 2287-237X (Print), 2287-2388 (Online)

scaffold materials are mainly composed of various types of materials, and can be combined with seed cells and bioactive substances. In the past decades, non-degradable metals such as titanium, titanium alloys, tantalum and cobalt-based alloys have been widely used in orthopedic implants. However, the main limitation of metals in clinical application at present lies in the serious stress shielding problem caused by their mechanical properties (Kannan and Raman 2008), and their non-degradability, which often requires secondary surgery to remove implants. More seriously, long-term corrosion or wear of some metal materials in the body will release toxic ions, such as titanium particles, and may even lead to inflammatory osteolysis (Puleo and Huh 1995, Jacobs *et al*. 2003). Therefore, if the above problems can be solved, metal materials can also become one of the osteochondral repair materials (Fazaeli *et al*. 2016, Ghazanfari *et al*. 2016, Habibi *et al*. 2016, 2018, Hosseini *et al*. 2018, Alipour *et al*. 2020, Cheshmeh *et al*. 2020, Ghabussi *et al*. 2020, Ghazanfari *et al*. 2020, Li *et al*. 2020a, b, Liu *et al*. 2020a, b, Moayedi *et al*. 2020c, Shariati *et al*. 2020b, Shi *et al*. 2020, Wang *et al*. 2020b).

Recently, more and more attention has been paid to biodegradable metal materials, among which magnesium (Mg) and magnesium alloys have become a new research hotspot (Witte *et al*. 2005, Zilberman and Eberhart 2006). This kind of material abandons the traditional idea that people usually use bio-inert materials as metal implant materials, and skillfully utilizes the corrosion characteristics of metal materials such as magnesium alloy in human environment to achieve the medical clinical purpose that metal implants gradually degrade in vivo until finally disappear (Azimi *et al*. 2016, Ebrahimi and Shafiei 2016, Ghadiri and Shafiei 2016a, b, c, Ghadiri *et al*. 2016a, b, c, d, Shafiei *et al*. 2016a, b, c, d, e, f, g). In addition, compared with biodegradable polymer materials such as polylactic acid in clinical application, magnesium alloy has more excellent metal material characteristics such as strong plasticity, stiffness and processability, so it has greater advantages as a hard tissue repair material such as bone. In recent years, JDBM alloy(Mg−Nd−Zn−Zr) developed by Shanghai Jiao Tong University (Mao *et al*. 2013, Zhang *et al*. 2016) which cooperated with our company, has better mechanical properties than the existing commercial magnesium alloys WE43 and AZ31, and has good biosafety, biodegradability and bone conductivity (Zhang *et al*. 2012b). Studies have shown that magnesium ions in magnesium alloys can promote chondrocyte proliferation. The research results of Dou *et al*. (2014) of Peking University suggest that Mg^{2+} can stimulate chondrocyte growth in a dose-dependent manner. Lozano *et al*. (2013) suggested that 10mM Mg^{2+} concentration can increase the proliferation of human articular chondrocytes, while 20mM Mg^{2+} concentration can inhibit the proliferation of chondrocytes, promote the differentiation of chondrocytes, and promote the expression of type II collagen and proteoglycan genes and proteins. JDBM alloy has been proved to have excellent osteogenic properties in vitro and in vivo (Wang *et al*. 2012, Kong *et al*. 2018), but its ability to repair osteochondral tissue in vivo and the mechanism leading to this effect have not been studied (Hamidi *et al*. 2015, Allahkarami *et al*. 2017, Ehyaei *et al*. 2017a, Akbas 2018a, b, Arefi and Zenkour 2018, Aydogdu *et al*. 2018, Bensaid *et al*. 2018, Navi *et al*. 2019, Ebrahimi *et al*. 2020, Gafour *et al*. 2020, Matouk *et al*. 2020a).

Many studies have shown that Wnt/β-catenin signal may play a unique role in joint tissue by controlling the functions of chondrocytes, osteoblasts and synoviocytes. Wnt/β-catenin signaling pathway family members are highly conserved secretory glycoproteins, which are closely related to cell proliferation, migration and differentiation (Pei *et al*. 2012). This pathway plays an important role in the maintenance of homeostasis in the internal environment, organ development and the occurrence of multiple system diseases, which is closely related to the physiological and pathological states of cartilage, bone and intervertebral disc (Ebrahimi and Shafiei 2017, Ebrahimi *et al*. 2017, Ehyaei *et al*. 2017b, Ghadiri *et al*. 2017a, b, c, d, e, Mirjavadi *et al*. 2017a, b, c, d, Shafiei and Kazemi 2017a, b, Shafiei *et al*. 2017a, b, c, d, 2019, 2020, Shivanian *et al*. 2017, Azimi *et al*. 2018, Shafiei and She 2018). However, the use of transforming growth factor (TGF) inhibitor in the nucleus of mouse related cells can block the entry of β-catenin into the nucleus, reduce its combination with lymphoid augmenter factor (LEF)/TCF complex, prevent the secretion of downstream factors, and cause chondrocyte apoptosis and cartilage tissue destruction (Zhu *et al*. 2008). COLLAGEN II-ICAT tr ansgenic mice have been prepared, which can specifically inhibit the conduction of β-catenin signal in chondrocytes. Delayed maturation of growth plate chondrocytes and destruction of articular cartilage were observed in these mice (Chen *et al*. 2008, Zhu *et al*. 2008). All these findings indicate that Wnt/β-catenin signaling pathway plays a key role in articular cartilage repair, and appropriate levels of β-catenin are necessary to maintain cartilage homeostasis. In this study, a hypothesis was proposed: JDBM alloy induces osteochondral defect repair through Wnt/β-catenin signaling pathway. ICRT3 [chemical name: 2-(((2-(4-Ethylphenyl)-5-methyl-1,3-oxazol-4-yl) methyl) sulfanyl)-N-(2-phenylethyl) acetamide], a small cell-permeable oxazole compound, was used as a selective inhibitor of the Wnt pathway by directly binding to β-catenin, thus blocking the interaction of β-catenin-TCF. It can be used to verify whether the hypothesis is true (Moayedi *et al*. 2020a, b, Oyarhossein *et al*. 2020, Shariati *et al*. 2020a, Zhou *et al*. 2020, Dai *et al*. 2021b, Guo *et al*. 2021, He *et al*. 2021, Hu *et al*. 2021, Huang *et al*. 2021a, Huo *et al*. 2021, Liu *et al*. 2021b, c, Peng *et al*. 2021, Shao *et al*. 2021, Zhang *et al*. 2021a, b).

2. Materials and method

2.1 Preparation of magnesium alloy samples and animal experimental design

A total of 54 healthy Sprague-Dawley (SD)rats, male, aged 6-8 weeks, were purchased from Zhuhai Baishitong Biotechnology Co., Ltd., with license No. SCXK (Guangdong) 2020-0051 and experimental unit license No.

Table 1 ICP-AES analyzed results of the chemical composition of JDBM

Alloy	Nd	Zn	Zr	Fe	Ni	Cu	Si	Mg
JDBM	3.130	0.164	0.413	0.003	0.001	0.001	0.003	Balance
Pure magnesium				≤0.0014	≤0.0001	≤0.0004	≤0.016	≥99.99

Table 2 Subject groups and study design.

Groups	No. of rats	Treatment
Control	18	Osteochondral defect model + Intraperitoneal injection of equal volume of saline as ICRT3 drugs(q.d)
JDBM	18	Osteochondral defect model + JDBM alloy sample + Intraperitoneal injection of equal volume of saline as ICRT3 drugs (q.d)
JDBM+ICRT3	18	Osteochondral defect model + JDBM alloy sample + Intraperitoneal injection of ICRT3 drugs(10mg/kg,q.d)

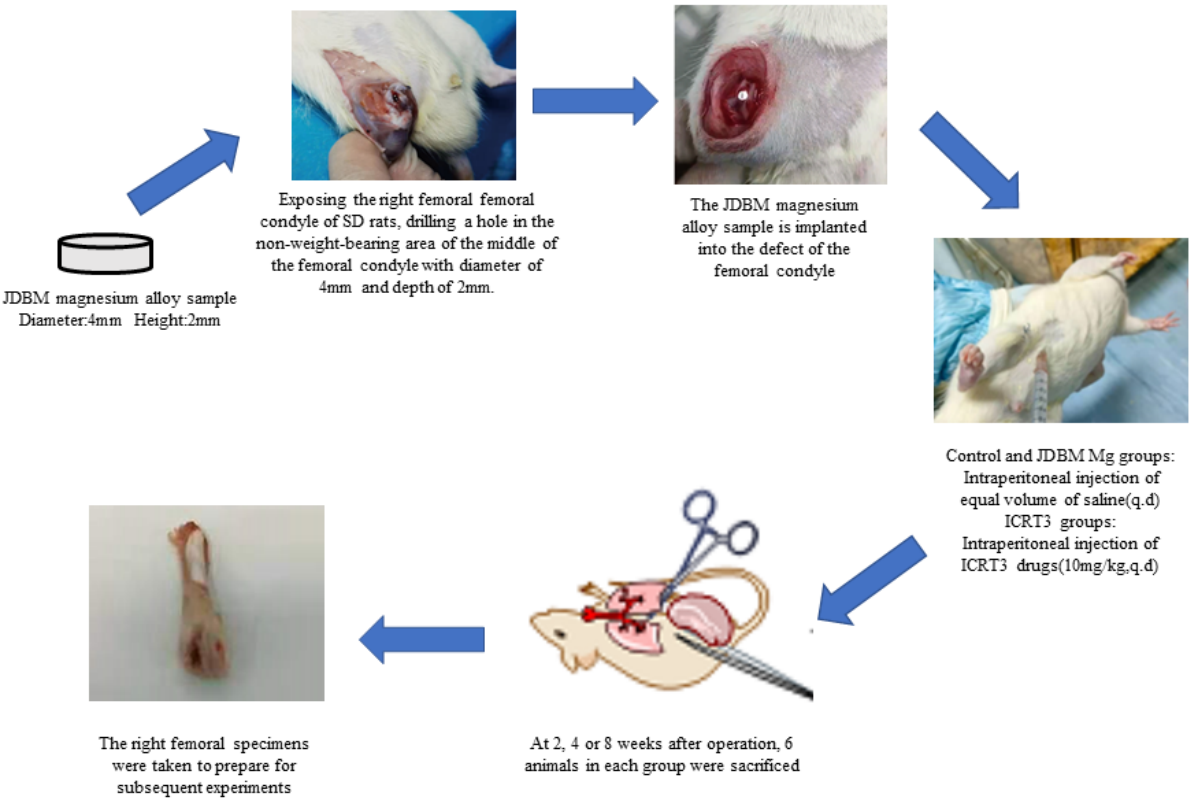

Fig. 1 Circulation of femoral condyle of rats

SYXK (Guangdong) 2020-0230. All experiments were carried out under the approval of the Animal Ethical Committee (Ethical approval number of this project: IACUC-2021-0076) and conformed with the guidelines of the National Institutes of Health for the Care and Use of Animals. JDBM alloy (PRC Patent Application No. 201010204719.9) bracket was provided by School of Materials, Shanghai Jiao Tong University. The chemical composition of the JDBM alloy is shown in Table 1.

JDBM alloy was prepared by semi-continuous casting with high purity Mg (≥99.99%), Zn (≥99.995%), Mg-25%Nd and Mg-30%Zr, which was detailed in previous report (Zhang *et al*. 2012a, b). In this experiment, JDBM alloy rod was machined into a small cylinder with a diameter of 4 mm and a height of 2 mm. The samples were mechanically polished to no. 7000 sandpaper and then ultrasonically cleaned in anhydrous ethanol for 10 minutes, then sterilized with ultraviolet radiation for 1 hour before in vivo testing (Chen *et al*. 2020). All rats were kept in Specific Pathogen Free (SPF)class animal room for 1 week at room temperature (24 ± 2) ℃, alternating day and night every 12 h, drinking water and eating freely. After quarantine, the animals were randomly divided into groups, and the grouping and treatment were as follows (Table 2).

After anesthesia, the right leg was selected as the experimental leg. After the defect in the non-weight-bearing area of the femoral condyle established by operation (holes with a diameter of 4mm and a depth of 3mm by bone drill, penetrating the subchondral bone and down into the marrow cavity), the Control group left the defect empty and did not

undergo any treatment, which was raised routinely after suture and disinfection, rats in JDBM group and JDBM+ ICRT3 group were anesthetized and punched in the same way to establish defects in the femoral condyle of rats, then filled with materials, sutured and disinfected, and then fed routinely (Fig. 1), after implantation, JDBM+ICRT3 group was injected intraperitoneally with ICRT3 drug 10 mg/kg once a day, and the other two groups were injected with the same amount of normal saline. At 2, 4 or 8 weeks after operation, 6 animals in each group were killed after cervical dislocation after anesthesia, and right femoral specimens were taken. Before euthanasia, rats were given intraperitoneal injection of 10% chloral hydrate (300 mg/kg) for general anesthesia. Then an experienced researcher performed the cervical dislocation very quickly, and no mice showed clinical signs of suffering before death. Samples were collected according to laboratory standards only after confirming that there was no heartbeat and their bodies became cold (Dai *et al*. 2021a, Ebrahimi *et al*. 2021, Hashemi *et al*. 2021, Hou *et al*. 2021, Huang *et al*. 2021b, c, Jiao *et al*. 2021, Liu *et al*. 2021a, d, Ma *et al*. 2021, Moradi *et al*. 2021, Najaafi *et al*. 2021, Shariati *et al*. 2021, Wu and Habibi 2021, Xu *et al*. 2021, Zhao *et al*. 2021, Yu *et al*. 2022).

2.2 Micro-computed tomography (CT) analysis

All samples were fixed in 4% paraformaldehyde at room temperature. A miniature CT machine (μ CT-80, SCANCO Medical) with a medium resolution (500 project/180 °) and a voxel size of 10 μ was used to scan meters in the axial direction parallel to the long axis of the sample. The system was set to 70 kV, 114 μA, 8W. The sagittal image of each sample was captured, and the femoral condyle of rats were delineated as the analysis region. The microstructural parameters of new bone were evaluated by using the software provided by the equipment, including the ratio of bone volume/total volume (BV/TV), the number of trabecula (Tb.N), the thickness of trabecula (Tb.Th) and the separation of trabecula (Tb.Sp).

2.3 Histological evaluation (HE) of osteochondral regeneration

The sections fixed with 4% paraformaldehyde were dehydrated, dyed with hematoxylin solution (Servicebio, China) for 5min, soaked in 1% acid-ethanol solution (1% hydrochloric acid-70% ethanol solution) for 5 times, washed with distilled water, dyed with eosin solution (Servicebio, China) for 3 min, dehydrated with different concentrations of alcohol, and washed with xylene. Then the slide was examined under Olympus BX53 fluorescence microscope to observe the tissue morphology.

2.4 Alizarin red staining of calcium nodules regeneration

According to the literature, osteogenic induction of cells may lead to mineralized nodules and calcium deposition, which can be determined by alizarin red staining (Samsa *et al*. 2016), so we performed alizarin red staining in this experiment. Specifically, sections fixed with 4% paraformaldehyde were dehydrated and then stained with 40 mM alizarin red staining solution (Biotia, U.S.A.) at 37°C for 1 hour to label calcium deposits. After that, all plates were rinsed with distilled water to wash the unbound alizarin red and scanned.

2.5 Masson staining evaluation of cartilage regeneration

In Masson's trichrome staining, tissue slices were first soaked in hematoxylin dye solution for 10min, and then washed with distilled water. Then soak the tissue for 10min with Ponceau Magenta dye solution. Finally, the tissue sections were soaked in aniline blue dye solution for 2min. All the above staining solutions were from Masson Trichrome Kit (ASPEN, U.S.A.). They were then examined with an OlympusBX53 microscope.

2.6 Real-time reverse transcription polymerase chain reaction (qRT-PCR) for specific gene expression

For the detection of signal pathway, osteogenesis and chondrogenesis related genes, the mortar was precooled with liquid nitrogen, and proper amount of tissue was broken in liquid nitrogen. The broken tissue was placed in a ribozyme-free 1.5 ml centrifuge tube preloaded with 150uL Buffer RZ (Tiangen, China) to extract total RNA, and cDNA was synthesized by reverse transcription using PrimeScript ™ RT Master Mix (Takara, Japan) based on the protocol of Manufacturer. Then, transcription levels were measured by qRT-PCR and SYBR Green PCR kit (Takara, Japan) using the ABI PRISM 7500 sequence detection system (Life Technologies Corporation, CA). The PCR reaction system consists of 1μl of cDNA of 10μl of S SYBR ® Premix Ex Taq (Takara, Japan) and 0.25 μ m of each pair of primers in a total volume of 20μl. The reaction conditions were as follows: initial denaturation at 95°C for 30 s, followed by 40 cycles at 95°C for 5 s, annealing at 55°C for 30 s, and extension at 72°C for 30 s (Li *et al*. 2016). The arithmetic formula (2-Δ Δ Ct method) was used to determine the relative change of gene expression relative to internal control β-actin (Livak and Schmittgen 2001). Primer sequences are shown in the Table 3.

2.7 Western Blot (WB) for specific protein expression

After removing blood stains, the condyles of femur tissue were cut into small pieces and placed in a homogenizer. Tissue protein extraction reagent (Tiangen, China), which is 10 times larger than the tissue volume, was added to ensure that the homogenate was completely cracked, and the supernatant was extracted, which was the total protein solution. The protein concentration was determined by BCA protein assay kit (Beyotime, China). The same amount of protein was separated by 10% SDS-PAGE and transferred to PVDF film. After blocking, the membrane binding protein and primary antibody were incubated overnight at 4 C. After washing and incubation with secondary antibody, protein levels were detected using enhanced chemiluminescence reagent (Millipore, U.S.A.).

Table 3 Primer sequences

Gene	Primer sequence (5′–3′)
β-actin	F: CACCAGGGTGTGATGGTG
	R: GTACATGGCTGGGGTGTTG
Wnt1	F: AACAGTAGTGGCCGATGGTG
	R: CGGAATTGCCACTTGCACTC
Wnt2	F: TCCTCCAGGGTGATGTGTGA
	R: GATGGCGTAAACAAAGGCCG
Wnt3a	F: ACCATGTTCGGGACCTATTCCA
	R: GCCTGTAGCATCTCGCTTCCA
β-catenin	F: AAGGTGCTGTCTGTCTGCTC
	R: GCTGCACTAGAGTCCCAAGG
Opn	F: CAGAACCAGTGTCTGGCAGT
	R: TCCTTTGTCTGCAGCACCTC
Ocn	F: ACTGCATTCTGCCTCTCTGAC
	R: CGCCGGAGTCTATTCACCAC
Runx2	F: CAGACACAATCCTCCCCACC
	R: GCCAGAGGCAGAAGTCAGAG
Bmp2	F: ACCCGCTGTCTTCTAGTGTTG
	R: AGCCTCAACTCAAACTCGCT
Collagen II	F: GCCAGGATGCCCGAAAATTAG
	R: GTCACCTCTGGGTCCTTGTTC
Aggrecan	F: GGAGAAGAGACCCAAACAGCA
	R: GGTGGCTCCATTCAGACAAG

The primary antibody was from ASPEM, U.S.A. (dilution 1: 1000). Antibodies against WNT3a, β-catenin, RUNX2 and BMP2 in the second antibody were derived from Abcam, U.S.A., anti-OCN and OPN antibodies were derived from Santa Cruz, U.S.A., anti-COLLAGEN II and AGGRECAN antibodies are from Proteintech, U.S.A., The anti-GAPDH antibody was purchased from Sigma-Aldrich, U.S.A. All impressions were exposed for visualization between 5 seconds and 2 min. The intensity of protein bands was quantified by ImageJ software (http://imagej.nih.gov/ij/download.html). The ratio of IntDen (protein)/IntDen (GAPDH) was calculated to ensure that the detected protein bands were linearized.

3. Statistical analysis

Statistical analyses were performed using GraphPad Prism 6.0 software. Each experiment was performed in triplicate with all the data expressed as the mean ± SD. Statistical differences used Student's t test and one-way analysis of variance (ANOVA). Values were considered statistically significant at $p < 0.05$.

4. Results

4.1 Micro-CT analysis of osteochondral regeneration

At 2, 4 and 8 weeks after operation, new bone formation was measured by micro CT (Figs. 2 and 3). From the results, the ratio of bone tissue volume to tissue volume in JDBM group was higher than that in Control group at 2 and 4 weeks, and the difference was statistically significant, At the 4th and 8th week, the number and thickness of trabecular bone in JDBM group were also significantly higher than those in Control group, These data showed that JDBM alloy implants have a large number of bones and obvious mineralization. Compared with the JDBM group, the bone parameters BV/TV, Tb. N, Tb. Th in JDBM+ ICRT3 group were lower than those in the Control group, but Tb. Sp in the 2nd and 8th week was higher than that in the JDBM group, which indicated that ICRT3 injection after JDBM alloy implantation could significantly inhibit bone regeneration.

4.2 Alizarin red staining evaluation of in vivo calcium nodules in defects

Alizarin red chelates with calcium ions to form a complex, which is used to identify the calcium salt components of tissues and cells, so we focus on observing the calcified layer of cartilage (Fig. 4). As shown in the figure, JDBM alloy showed strong mineralization promotion ability after implantation, and calcium nodules were formed in the second week, while a large number of calcium nodules were formed in the eighth week, and the whole tissue was stained deeply. However, the content of calcium nodules in Control group was less at the 2 and 4 weeks, and a large number of calcium nodules were produced at the 8th week. It could be seen that JDBM alloy can promote mineralization and accelerate the repair of defects in early stage. However, in the JDBM+ICRT3 group, it was difficult to see obvious calcium nodules at the 2nd and 4th weeks, and sporadic calcium nodules began to appear at the 8th week. It can be seen that ICRT3 has a strong inhibitory effect on the mineralization promotion of JDBM alloy. Together, these results indicated that JDBM alloy promoted osteogenesis and that was blocked by ICRT3.

4.3 Masson staining evaluation of in vivo cartilage regeneration in defects

From Masson staining, we can clearly see the gradual transformation of cartilage defect repair from basic fibrous tissue to cartilage-like tissue in rats (Fig. 5). At the 2 weeks, the cartilage layers of the three groups were filled with a large number of fibroblasts, at the 4 weeks group, the JDBM group had more cartilage-like tissue formed, in contrast, defects at 8 weeks presented with more cartilage-like tissue proliferating from the bottom and decreased fibrous contents, and the chondrocytes are arranged in a typical manner. However, the JDBM+ICRT3 drug group always had a large number of fibroblast tissues. These data suggested that JDBM alloy enhanced chondrogenesis which could be inhibited by ICRT3.

4.4 qRT-PCR evaluation of in vivo osteochondral regeneration in defects

The genes of *Wnt1*, *Wnt2*, *Wnt3a*, *β-catenin*, *Runx2*, *Bmp2*, *Opn*, *Ocn* and chondrogenesis gene *Collagen II*,

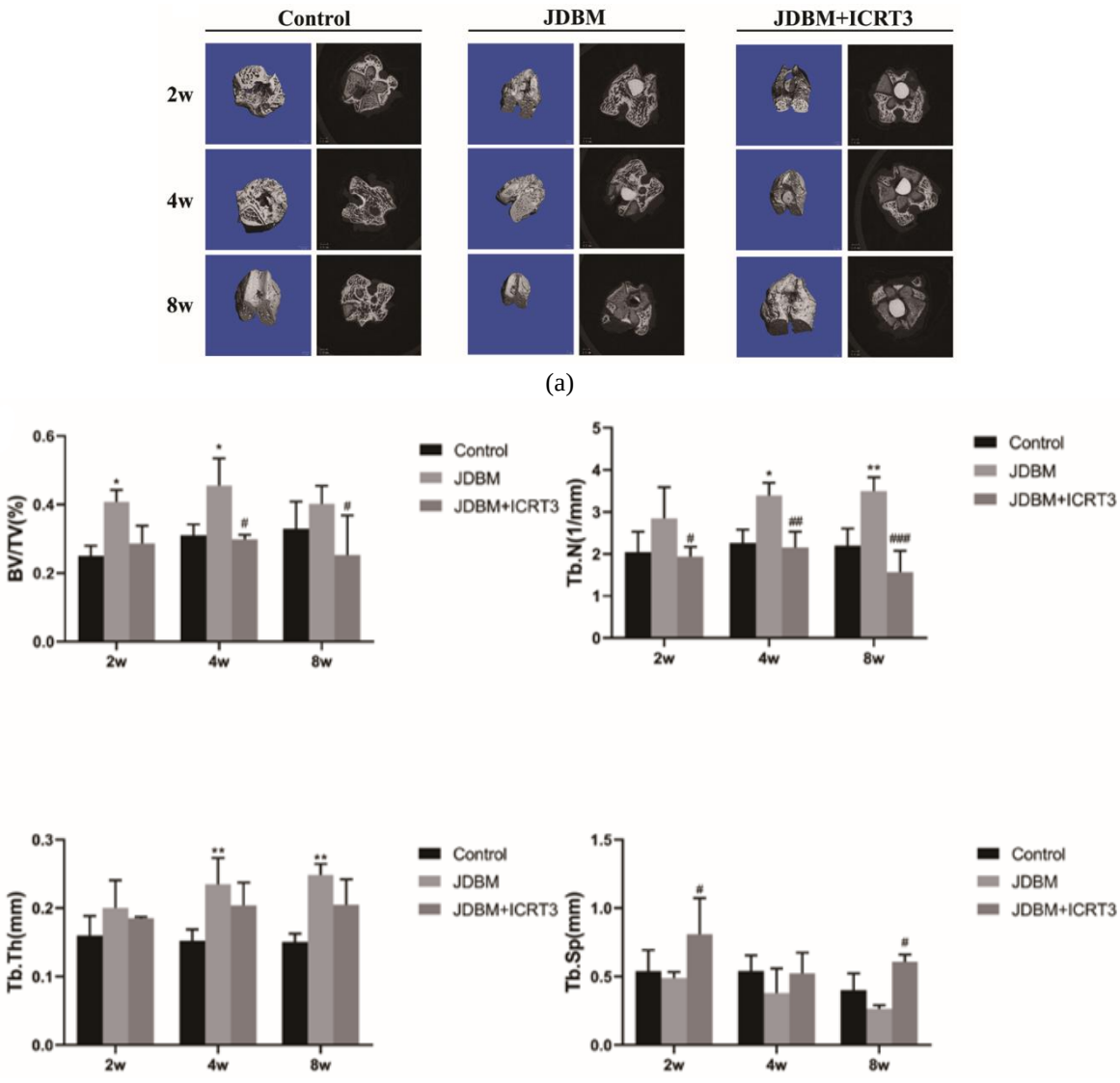

(a)

(b)

Fig. 2 The measured new bone foundation

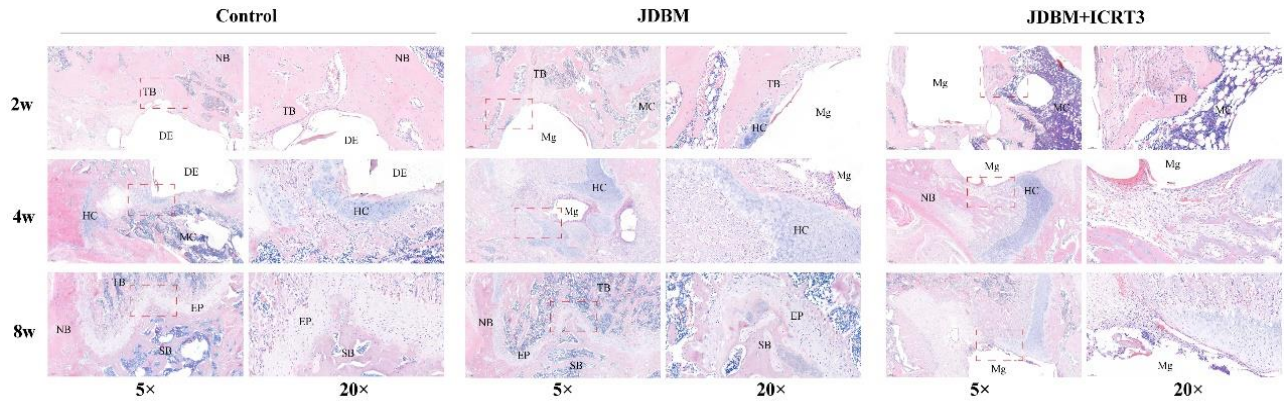

Fig. 3 Graphic of new bone foundation

Aggrecan were detected by qRT-PCR (Table 4). The results in Fig. 6 showed that the signaling pathway genes *Wnt3a* and *β-catenin* were significantly increased in JDBM group at the fourth week, while the signaling pathway was inhibited and the expression of *Wnt3a* and *β-catenin* was decreased in JDBM+ICRT3 group after JDBM alloy implantation. *Wnt3a* was statistically significant at the fourth week, and β-catenin showed low expression at the

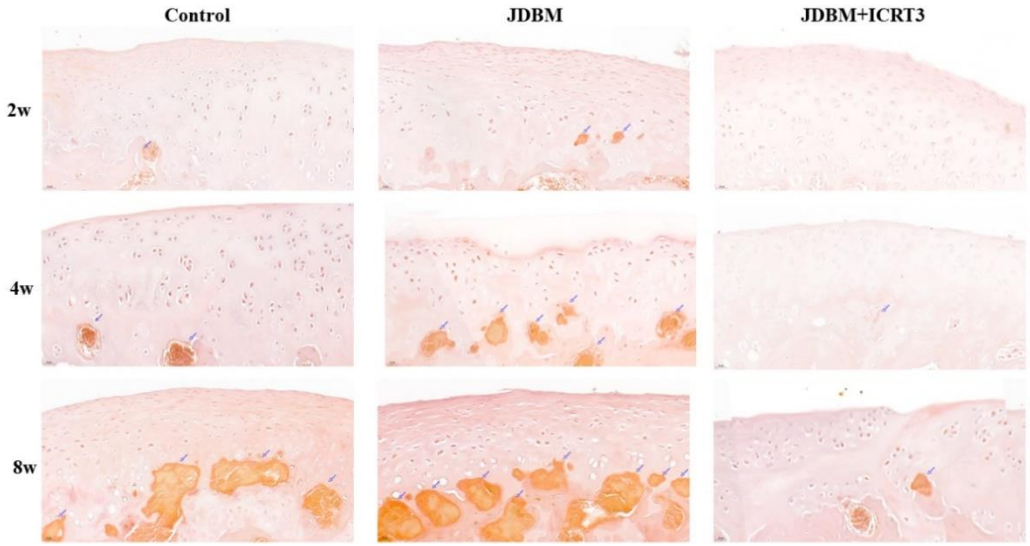

Fig. 4 Graphic and control of bone foundation

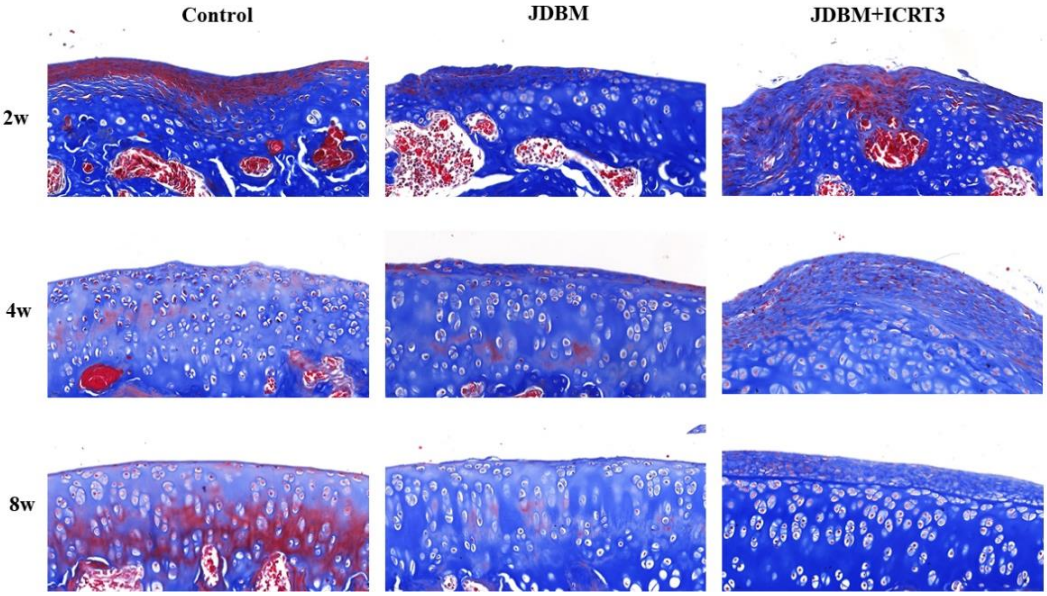

Fig. 5 Transformation of cartilage defect repair

Table 4 The results of qRT-PCR

Groups / Weeks	Control	JDBM	JDBM+ICRT3	Control	JDBM	JDBM+ICRT3
		Wnt1			Ocn	
2	1.000±0.026	0.960±0.087	0.947±0.031	0.997±0.015	1.153±0.006	0.823±0.049
4	1.000±0.050	1.017±0.006	0.553±0.025	1.000±0.000	1.873±0.006	1.080±0.020
8	1.000±0.070	1.140±0.020	0.510±0.020	1.003±0.006	1.123±0.042	0.370±0.010
		Wnt2			Runx2	
2	1.003±0.098	0.770±0.061	0.873±0.060	1.000±0.020	1.740±0.036	0.887±0.021
4	1.000±0.072	0.633±0.042	0.413±0.031	1.000±0.030	1.730±0.046	0.857±0.021
8	1.000±0.070	0.947±0.075	0.643±0.047	1.000±0.010	0.937±0.006	0.637±0.012
		Wnt3a			Bmp2	
2	1.000±0.053	0.990±0.105	0.857±0.061	1.000±0.017	1.530±0.017	0.937±0.057
4	1.620±0.848	3.133±0.562	1.207±0.321	1.003±0.038	1.953±0.021	1.100±0.000
8	1.180±0.252	1.260±0.168	0.543±0.295	1.000±0.000	0.880±0.010	0.497±0.006

Table 4 Continued

Groups / Weeks	Control	JDBM	JDBM+ICRT3	Control	JDBM	JDBM+ICRT3
	Wnt1			Ocn		
	β-catenin			Collagen II		
2	1.000±0.050	1.397±0.021	0.910±0.106	1.033±0.035	1.253±0.012	0.927±0.040
4	1.000±0.017	1.450±0.017	0.807±0.012	1.000±0.010	1.940±0.020	0.713±0.006
8	1.000±0.010	1.237±0.189	0.653±0.006	1.000±0.010	0.883±0.367	0.497±0.023
	Opn			Aggrecan		
2	1.003±0.064	1.167±0.032	0.863±0.083	1.000±0.026	2.140±0.035	0.917±0.093
4	1.003±0.006	1.620±0.050	0.810±0.010	1.000±0.095	2.623±0.085	1.433±0.046
8	1.000±0.010	1.023±0.067	0.667±0.012	1.000±0.053	0.803±0.049	0.680±0.010

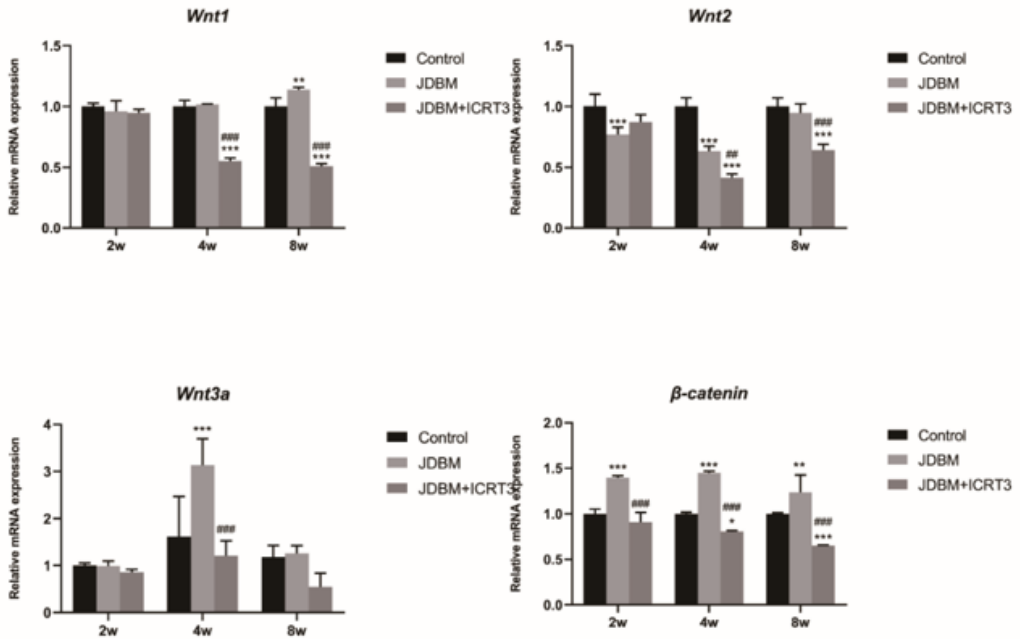

(a)

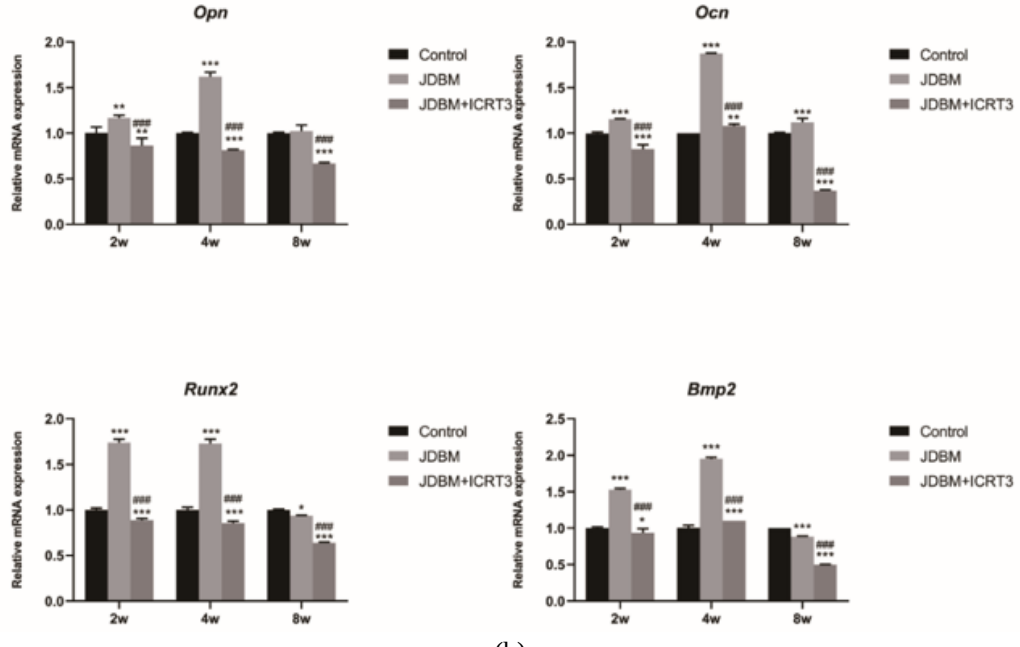

(b)

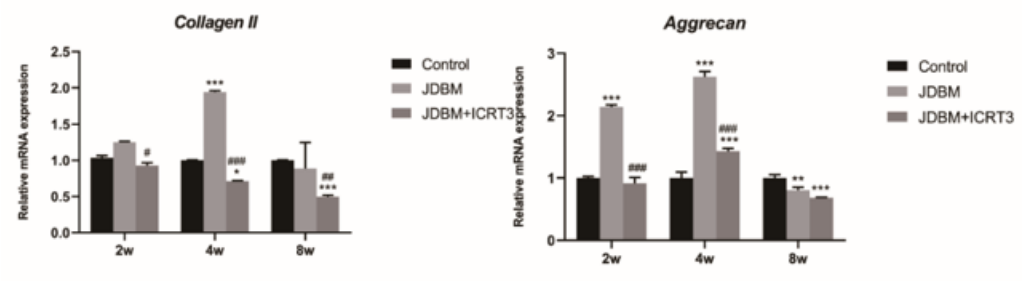

(c)

Fig. 6 Signaling pathway genes

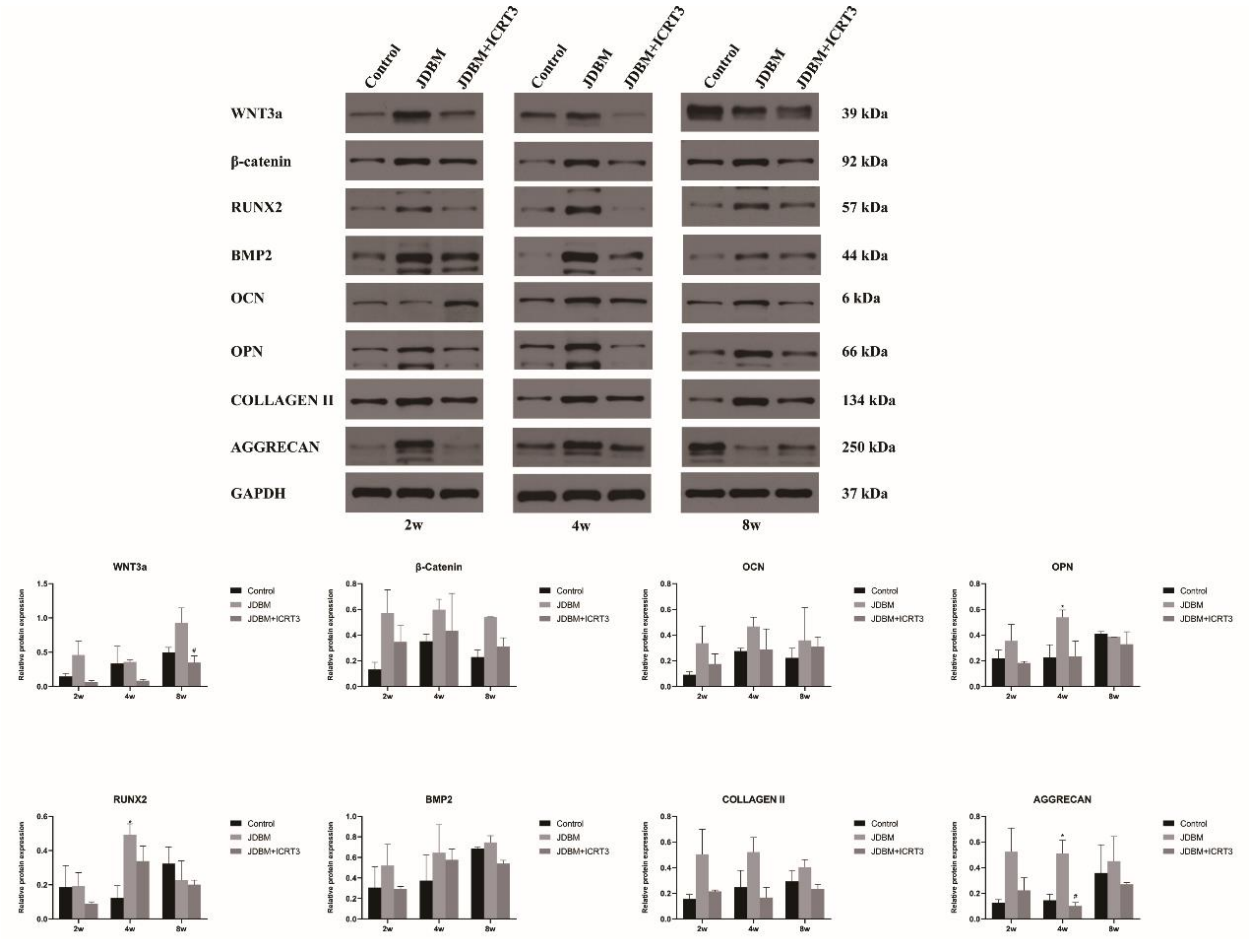

Fig. 7 The expression of WNT3a protein at the eighth week and AGGRECAN protein at the fourth week

second, fourth and eighth weeks. The osteogenesis-related genes *Runx2*, *Bmp2*, *Opn and Ocn* in the JDBM group showed high expression, especially in the 4th week, the expression level was significantly higher than that in the Control group. At the 8th week, with the gradual improvement of tissue repair, the difference of osteogenesis gene expression in JDBM group was reduced or even eliminated compared with that in the Control group. However, in JDBM+ICRT3 group, the expression of osteogenesis genes was still at a low level because of continuous use of signal pathway blockers. We also detected chondrogenesis genes *Collagen II* and *Aggrecan*. It was gratifying that JDBM group also showed excellent results in cartilage formation. The expression of *Collagen II* in the fourth week and *Aggrecan* in the second and fourth weeks was much higher than that in the Control group, but there was no statistical difference between them in the eighth week. The gene expression of JDBM+ICRT3 group was always at a low level during the observation period.

4.5 Western blot evaluation of in vivo osteochondral regeneration in defects

Through WB detection for WNT3a, β-catenin, RUNX2, BMP2, OCN, OPN, COLLAGEN II, AGGRECAN, it could be seen from WB detection that JDBM group protein

expression was higher than the other two groups, but only RUNX2, OPN, AGGRECAN protein at the 4th week showed statistical differences (Fig. 7). The expression of WNT3a protein at the eighth week and AGGRECAN protein at the fourth week was significantly lower than that in JDBM group. The expression of WNTt3a protein at the 8th week and AGGRECAN protein at the 4th week was significantly lower than that in JDBM group.

5. Discussion

This study aimed to repair osteochondral defects with JDBM alloy and detected whether the repair was mediated by Wnt/β-catenin signaling pathway. JDBM alloy has been proved to have good biocompatibility and osteogenic and cartilaginous characteristics in vitro in the early stage, and some experiments have shown that JDBM alloy can repair bone defects in vivo (Wang *et al*. 2012, 2020a, Zhang *et al*. 2012b). So far, there was no study on its repair effect and mechanism on osteochondral tissue. In this study, a rat model of osteochondral defect was established and specific Wnt/β-catenin inhibitor ICRT3 was injected. The research showed that JDBM alloy is more helpful to repair osteochondral defects, and the repair effect depended on Wnt/β-catenin signaling pathway.

In this study, the effects of blank group, JDBM group and JDBM+ICRT3 group on the repair of osteochondral defects in rats were explored. MicroCT quantitative analysis showed that the data of BV/TV, Tb.N and Tb.Th of JDBM alloy were higher than that of Control group at the 4th week, However, there was no statistical difference between the JDBM+ICRT3 and the Control group. Compared with JDBM group, BV/TV and Tb.N in JDBM+ICRT3 group decreased at the 4th and 8th weeks, while Tb.Sp increased at the 2nd and 8th weeks. We can see that most of the defects have been repaired in JDBM group at the 4th week by HE section staining of three groups. In addition, there are a large number of overgrown chondrocytes around the defect. In the same period, the defect of Control group is gradually repaired, and a small number of chondrocytes are gathered. However, compared with the previous two groups, the defect of JDBM+ICRT3 group in this period is still larger and the repair is slow. At the 8th week, we can see that the defects in Control group and JDBM group were almost completely repaired, and the epiphyseal plates were continuous. There are abundant trabeculae in new bone, but there are still large defects in JDBM+ICRT3 group that have not been repaired. The same situation can be seen in alizarin red staining. The content of calcium nodules in JDBM group was higher than that in the other two groups during the observation period, and the calcium nodules stained deeply and continuously at the 8th week. In Control group, a small amount of calcium nodules were also produced at the 2nd and 4th weeks, and the content was greatly higher at the 8th week. However, in JDBM+ICRT3 group, there were almost no calcium nodules at the 2nd and 4th weeks, and a few calcium nodules could be seen until the 8th week. The results of Masson staining show that in the 4th week group, more cartilage-like tissues were formed in the JDBM group, and more cartilage-like tissues proliferated from the bottom at the 8th week, with reduced fiber content and typical chondrocyte arrangement. The JDBM+ICRT3 group always had more fibrous tissue. From the above histological staining, we can see that compared with Control group, JDBM group began to form new bone tissue at an early stage, which is helpful for osteogenesis and mineralization of stem cells. However, after ICRT3 was added, the effect of JDBM alloy was counteracted, and there was no obvious osteogenesis or chondrogenesis at 2, 4 and 8 weeks. It can be seen that the action of JDBM alloy depends on Wnt/β-catenin signaling pathway.

We used qRT-PCR technology to detect a variety of genes in the samples. Among them, the *Runx2* gene is a specific transcription factor for osteoblasts, which plays an important role in the formation and reconstruction of bone tissue, *Bmp2* is a bone morphogenetic protein gene, which has the strongest bone formation effect among all the known growth factors, and has the ability to promote the directional differentiation and proliferation of mesenchymal stem cells into osteoblasts, *Ocn* is human osteocalcin, which can reflect the activity of osteoblasts or bone formation, and is an indicator of bone formation, *Opn* is osteopontin, which is widely present in mature bone tissues. *Collagen II* and *Aggrecan* are the main components of the extrachondral matrix, secreted by chondrocytes, and are important signs of cartilage formation. The results of qRT-PCR showed that compared with Control group, the osteogenesis-related gene *Runx2*, *BMP2*, *OCN* and *OPN* in JDBM group were increased in different degrees in 2, 4 and 8, and the chondrogensis genes *Collagen II* and *Aggrecan* were also increased, which indicated that JDBM alloy had a positive effect on repairing cartilage defects in rats. In JDBM+ ICRT3 group, osteogenesis and chondrogenesis related genes decreased compared with JDBM group, so ICRT3 inhibited the effect of JDBM alloy. After detecting the related factors *Wnt1*,*Wnt2*,*Wnt3a and β-catenin* of Wnt/β-catenin signaling pathway, it is found that after ICRT3 was added, these genes decreased compared with JDBM group, among which *Wnt3a* decreased most at the 4th week, and *β-catenin* gene also expressed at a low level at the 2nd, 4th and 8th weeks, which was lower than that of Control group. In the results of WB, RUNX2, OPN and AGGRECAN were increased in JDBM group at the fourth week, while other factors were not statistically significant in WB. From the results of qRT-PCR and WB, we could conculde that JDBM alloy activated the transcription and expression of osteogenic and chondrogenic genes at an earlier stage than the Control group. A previous genome-wide association study of GWAS showed that many members of Wnt/β-catenin signaling pathway are related to bone mineral density and fracture susceptibility (Hsu and Kiel 2012). In the early stage of fracture repair, pluripotent mesenchymal stem cells differentiate into osteoblasts or chondrocytes by activating β-catenin protein, and in the later stage of repair, proosteoblasts also need to differentiate into osteoblasts by activating β-catenin protein (Chen *et al*. 2007). Hung *et al*. (2019) found that additional 10mM magnesium ions activate the classical signaling pathway Wnt. It can also significantly increase the expression of β-catenin and its

downstream genes (LEF1 and DKK1), and then lead human bone marrow stromal cell to differentiate into osteoblasts and produce osteogenesis. In this study, we also verified the same results. Bone and cartilage defects are difficult to repair after inhibiting Wnt/β-catenin signaling pathway. This shows that this signal pathway plays an important role in promoting bone and cartilage formation.

Coincidentally, Wang *et al*. (2020a) verified at the cellular level that JDBM alloy can stimulate osteogenic differentiation of bone marrow mesenchymal stem cells in vitro, the study shows that compared with cells inoculated on pure magnesium samples, osteoblasts cultured on JDBM alloy samples show better cell adhesion, improved cell proliferation and increased mineralization ability (Kong *et al*. 2018), Liao *et al*. (2015) shows that JDBM alloy is beneficial to the adhesion and proliferation of chondrocytes. This study had verified in vivo experiments that JDBM alloy stimulates the expression of osteogenic and chondrogenic genes and proteins. From the results of histology and molecular biology, we could find that JDBM alloy had a strong effect on the repair of bone tissue. However, the cartilage tissue repair effect had not reached the ideal state. The newly generated cartilage tissue was still fibrocartilage instead of hyaline cartilage. From the Masson staining, the cartilage fibers formed by the JDBM group were more arranged ordered and dense. However, it was encouraging that the JDBM alloy helped the repair of subchondral bone. Previous studies have confirmed that the repair of subchondral bone was a necessary condition for cartilage growth. The rapidly healed subchondral bone helped repair the cartilage layer (Goldring and Goldring 2010, Li *et al*. 2013). Combining the results of microCT and HE staining, we could concluded that the subchondral bone repair of the JDBM group was more complete than that of the Control group, and the bone trabeculae were arranged neatly and densely, which indicates that the JDBM alloy repaired the subchondral bone in terms of excellent performance, we could use the characteristics of JDBM alloy to conduct in-depth research, hoping to find a way to make new cartilage into hyaline cartilage.

In the course of this study, three key osteogenesis-related proteins in the three groups have similar expression profiles. OCN OPN and BMP2 are markers of osteoblasts secreted mainly by osteoblasts and the proportion of positive cells represents the number and viability of osteoblasts which further indicates that the osteogenic effect is better in vivo. Combined with the results of HE and microCT analysis may prove the regulatory role of JDBM alloy in bone formation. The expression of OCN, OPN and BMP2 peaked at the 4th week after operation, and they reached very low levels at the 8th week after operation. Similarly, the chondrogenesis proteins AGGRECAN and COLLAGEN II also showed the same trend, reaching a high value at the 4th week, while the expression level decreased at the 8th week. It has been reported that magnesium ions released during the degradation of JDBM alloy can stimulate osteogenesis and chondrogensis. XU J research proves that the osteogenesis of magnesium can directly affect bone cells. Extracellular Mg^{2+} enters bone cells through magnesium channels/transports. This leads to the activation of ATF4-dependent Wnt/β-catenin signal in bone cells, which leads to the subsequent increase of intracellular cAMP level and the activation of bone repair related genes (Xu *et al*. 2022). However, Mg^{2+} deficiency (about 0.04-10%) can promote osteoclast formation (Belluci *et al*. 2013). Compared with PLGA scaffold, porous 3D PLGA/Mg (OH) scaffold manufactured by Park *et al*. (2018) can enhance the formation of cartilage markers, inhibit the release of inflammatory cytokines, reduce cell death and calcification, and increase the expression of COLLAGEN II at the 4th and 8th weeks. Mg^{2+} released during the degradation of the scaffold can support cartilage differentiation without inflammation and further calcification. These results indicate that magnesium ions in scaffolds can support cartilage healing by reducing calcification. Therefore, Mg^{2+} supplementation can not only enhance osteogenic repair, but also improve cartilage healing, which is also verified by our research.

6. Conclusions

In conclusion, the present study revealed that JDBM alloy promoted the repair of bone defects and cartilage defects in rats through Wnt/β-catenin signaling pathway. Thus, our findings suggest that JDBM alloy may serve as a potential therapeutic agent for the treatment of osteochondral defect.

Acknowledgement

This study was supported by grants from National Natural Science Foundation of China (No. 82172432, 82102568 and 82001319), National & Local Joint Engineering Research Center of Orthopaedic Biomaterials (No. XMHT20190204007), Shenzhen High-level Hospital Construction Fund, Shenzhen Key Medical Discipline Construction Fund (No. SZXK023), Shenzhen "San-Ming" Project of Medicine (No. SZSM201612092), Guangdong Basic and Applied Basic Research Foundation (No. 2021A1515012586 and 2019A1515011290), Bethune Charitable Foundation and CSPC Osteoporosis Research Foundation Project (No. G-X-2020-1107-21), Shenzhen Research and Development Projects (No. JCYJ20210318153832004), Sustainable development project of Science and Technology in Shenzhen (No. KCXFZ20201221173411031), and Scientific Research Foundation of PEKING UNIVERSITY SHENZHEN HOSPITAL (No. KYQD2021099).

References

Akbas, S.D. (2018a), "Forced vibration analysis of cracked functionally graded microbeams", *Adv. Nano Res.*, **6**(1), 39-55. http://doi.org/10.12989/anr.2018.6.1.039.

Akbas, S.D. (2018b), "Bending of a cracked functionally graded nanobeam", *Adv. Nano Res.*, **6**(3), 219-242. http://doi.org/10.12989/anr.2018.6.3.219.

Alipour, M., Torabi, M.A., Sareban, M., Lashini, H., Sadeghi, E., Fazaeli, A., Habibi, M. and Hashemi, R. (2020), "Finite element

and experimental method for analyzing the effects of martensite morphologies on the formability of DP steels", *Mech. Based Des. Struct.*, **48**(5), 525-541. http://doi.org/10.1080/15397734.2019.1633343.

Allahkarami, F., Nikkhah-Bahrami, M. and Saryazdi, M.G. (2017), "Damping and vibration analysis of viscoelastic curved microbeam reinforced with FG-CNTs resting on viscoelastic medium using strain gradient theory and DQM", *Steel Compos. Struct.*, **25**(2), 141-155. https://doi.org/10.12989/scs.2017.25.2.141.

Arefi, M. and Zenkour, A.M. (2018), "Free vibration analysis of a three-layered microbeam based on strain gradient theory and three-unknown shear and normal deformation theory", *Steel Compos. Struct.*, **26**(4), 421-437. https://doi.org/10.12989/scs.2018.26.4.421.

Aydogdu, M., Arda, M. and Filiz, S. (2018), "Vibration of axially functionally graded nano rods and beams with a variable nonlocal parameter", *Adv. Nano Res.*, **6**(3), 257-278. http://doi.org/10.12989/anr.2018.6.3.257.

Azimi, M., Mirjavadi, S.S., Shafiei, N. and Hamouda, A.M.S. (2016), "Thermo-mechanical vibration of rotating axially functionally graded nonlocal Timoshenko beam", *Appl. Phys. A*, **123**(1), 104. http://doi.org/10.1007/s00339-016-0712-5.

Azimi, M., Mirjavadi, S.S., Shafiei, N., Hamouda, A.M.S. and Davari, E. (2018), "Vibration of rotating functionally graded Timoshenko nano-beams with nonlinear thermal distribution", *Mech. Adv. Mater. Struct.*, **25**(6), 467-480. http://doi.org/10.1080/15376494.2017.1285455.

Baumann, C.A., Hinckel, B.B., Bozynski, C.C. and Farr, J. (2019), *Articular cartilage: Structure and restoration* in *Joint Preservation of the Knee*, Springer Cham, Denmark.

Belluci, M.M., Schoenmaker, T., Rossa-Junior, C., Orrico, S.R., de Vries, T.J. and Everts, V. (2013), "Magnesium deficiency results in an increased formation of osteoclasts", *J. Nutr. Biochem.*, **24**(8), 1488-1498. http://doi.org/10.1016/j.jnutbio.2012.12.008.

Bensaid, I., Bekhadda, A. and Kerboua, B. (2018), "Dynamic analysis of higher order shear-deformable nanobeams resting on elastic foundation based on nonlocal strain gradient theory", *Adv. Nano Res.*, **6**(3), 279-298. http://doi.org/10.12989/anr.2018.6.3.279.

Besseghier, A., Heireche, H., BoU.S.A.hla, A.A., Tounsi, A. and Benzair, A. (2015), "Nonlinear vibration properties of a zigzag single-walled carbon nanotube embedded in a polymer matrix", *Adv. Nano Res.*, **3**(1), 29-37. https://doi.org/10.12989/anr.2015.3.1.029.

Bouadi, A., BoU.S.A.hla, A.A., Houari, M.S.A., Heireche, H. and Tounsi, A. (2018), "A new nonlocal HSDT for analysis of stability of single layer graphene sheet", *Adv. Nano Res.*, **6**(2), 147-162. https://doi.org/10.12989/anr.2018.6.2.147.

Boutaleb, S., Benrahou, K.H., Bakora, A., Algarni, A., BoU.S.A.hla, A.A., Tounsi, A., Tounsi, A. and Mahmoud, S. (2019), "Dynamic analysis of nanosize FG rectangular plates based on simple nonlocal quasi 3D HSDT", *Adv. Nano Res.*, **7**(3), 191-208. https://doi.org/10.12989/anr.2019.7.3.191.

Chen, Y., Whetstone, H.C., Lin, A.C., Nadesan, P., Wei, Q., Poon, R. and Alman, B.A. (2007), "Beta-catenin signaling plays a disparate role in different phases of fracture repair: implications for therapy to improve bone healing", *PLoS Med.* **4**(7), e249. http://doi.org/10.1371/journal.pmed.0040249.

Chen, M., Zhu, M., Awad, H., Li, T.F., Sheu, T.J., Boyce, B.F., Chen, D. and O'Keefe, R.J. (2008), "Inhibition of beta-catenin signaling causes defects in postnatal cartilage development", *J. Cell Sci.* **121**(9), 1455-1465. http://doi.org/10.1242/jcs.020362.

Chen, S., Yu, L., Zhao, Q., Ren, Y., Guo, L., Gong, X., Wan, X., Yuan, G. and Li, B. (2020), "Comparative assessment of the biocompatibility and degradation behavior of Zn-3Cu and JDBM alloys used for biliary surgery", *Am. J. Transl. Res.*, **12**(1), 19-31.

Cheshmeh, E., Karbon, M., Eyvazian, A., Jung, D.w., Habibi, M. and Safarpour, M. (2020), "Buckling and vibration analysis of FG-CNTRC plate subjected to thermo-mechanical load based on higher order shear deformation theory", *Mech. Based Des. Struct.*, 1-24. http://doi.org/10.1080/15397734.2020.1744005.

Dai, Z., Jiang, Z., Zhang, L. and Habibi, M. (2021a), "Frequency characteristics and sensitivity analysis of a size-dependent laminated nanoshell", *Adv. Nano Res.*, **10**(2), 175-189. http://doi.org/10.12989/ANR.2021.10.2.175.

Dai, Z., Zhang, L., Bolandi, S.Y. and Habibi, M. (2021b), "On the vibrations of the non-polynomial viscoelastic composite open-type shell under residual stresses", *Compos. Struct.*, **263**, 113599. https://doi.org/10.1016/j.compstruct.2021.113599.

Dou, Y., Li, N., Zheng, Y. and Ge, Z. (2014), "Effects of fluctuant magnesium concentration on phenotype of the primary chondrocytes", *J. Biomed. Mater. Res. A*, **102**(12), 4455-4463. http://doi.org/10.1002/jbm.a.35113.

Ebrahimi, F. and Shafiei, N. (2016), "Application of Eringen's nonlocal elasticity theory for vibration analysis of rotating functionally graded nanobeams", *Smart Struct. Syst.*, **17**(5), 837-857. https://doi.org/10.12989/sss.2016.17.5.837.

Ebrahimi, F. and Shafiei, N. (2017), "Influence of initial shear stress on the vibration behavior of single-layered graphene sheets embedded in an elastic medium based on Reddy's higher-order shear deformation plate theory", *Mech. Adv. Mater. Struct.*, **24**(9), 761-772. http://doi.org/10.1080/15376494.2016.1196781.

Ebrahimi, F., Shafiei, N., Kazemi, M. and MoU.S.A.vi Abdollahi, S.M. (2017), "Thermo-mechanical vibration analysis of rotating nonlocal nanoplates applying generalized differential quadrature method", *Mech. Adv. Mater. Struct.*, **24**(15), 1257-1273. http://doi.org/10.1080/15376494.2016.1227499.

Ebrahimi, F., Kokaba, M., Shaghaghi, G. and Selvamani, R. (2020), "Dynamic characteristics of hygro-magneto-thermo-electrical nanobeam with non-ideal boundary conditions", *Adv. Nano Res.*, **8**(2), 169-182. https://doi.org/10.12989/anr.2020.8.2.169.

Ebrahimi, F., Mohammadi, K., Barouti, M.M. and Habibi, M. (2021), "Wave propagation analysis of a spinning porous graphene nanoplatelet-reinforced nanoshell", *Wave. Random Complex Med.*, **31**(6), 1655-1681. http://doi.org/10.1080/17455030.2019.1694729.

Ehyaei, J., Akbarshahi, A. and Shafiei, N. (2017a), "Influence of porosity and axial preload on vibration behavior of rotating FG nanobeam", *Adv. Nano Res.*, **5**(2), 141-169. http://doi.org/10.12989/anr.2017.5.2.141.

Ehyaei, J., Akbarshahi, A. and Shafiei, N. (2017b), "Influence of porosity and axial preload on vibration behavior of rotating FG nanobeam", **5**(2), 141-169. https://doi.org/10.12989/anr.2017.5.2.141.

Fazaeli, A., Habibi, M. and Ekrami, A.A. (2016), "Experimental and finite element comparison of mechanical properties and formability of dual phase steel and ferrite - pearlite steel with the same chemical composition %J Metallurgical Engineering", *Metall. Eng.*, **19**(2), 84-93. http://doi.org/10.22076/me.2017.41458.1064.

Felson, D.T., Lawrence, R.C., Dieppe, P.A., Hirsch, R., Helmick, C.G., Jordan, J.M., Kington, R.S., Lane, N.E., Nevitt, M.C., Zhang, Y., Sowers, M., McAlindon, T., Spector, T.D., Poole, A.R., Yanovski, S.Z., Ateshian, G., Sharma, L., Buckwalter, J.A., Brandt, K.D. and Fries, J.F. (2000), "Osteoarthritis: New insights. Part 1: The disease and its risk factors", *Ann. Intern. Med.* **133**(8), 635-646. http://doi.org/10.7326/0003-4819-133-8-200010170-00016.

Gafour, Y., Hamidi, A., Benahmed, A., Zidour, M. and Bensattalah, T. (2020), "Porosity-dependent free vibration

analysis of FG nanobeam using non-local shear deformation and energy principle", *Adv. Nano Res.*, **8**(1), 37-47. https://doi.org/10.12989/anr.2020.8.1.037.

Ghabussi, A., Habibi, M., NoormohammadiArani, O., Shavalipour, A., Moayedi, H. and Safarpour, H. (2020), "Frequency characteristics of a viscoelastic graphene nanoplatelet–reinforced composite circular microplate", *J. Vib. Control*, **27**(1-2), 101-118. http://doi.org/10.1177/1077546320923930.

Ghadiri, M. and Shafiei, N. (2016a), "Nonlinear bending vibration of a rotating nanobeam based on nonlocal Eringen's theory using differential quadrature method", *Microsyst. Technol.*, **22**(12), 2853-2867. http://doi.org/10.1007/s00542-015-2662-9.

Ghadiri, M. and Shafiei, N. (2016b), "Vibration analysis of a nano-turbine blade based on Eringen nonlocal elasticity applying the differential quadrature method", *J. Vib. Control*, **23**(19), 3247-3265. http://doi.org/10.1177/1077546315627723.

Ghadiri, M. and Shafiei, N. (2016c), "Vibration analysis of rotating functionally graded Timoshenko microbeam based on modified couple stress theory under different temperature distributions", *Acta Astronaut.*, **121**, 221-240. https://doi.org/10.1016/j.actaastro.2016.01.003.

Ghadiri, M., Hosseini, S.H.S. and Shafiei, N. (2016a), "A power series for vibration of a rotating nanobeam with considering thermal effect", *Mech. Adv. Mater. Struct.*, **23**(12), 1414-1420. http://doi.org/10.1080/15376494.2015.1091527.

Ghadiri, M., Shafiei, N. and Akbarshahi, A. (2016b), "Influence of thermal and surface effects on vibration behavior of nonlocal rotating Timoshenko nanobeam", *Appl. Phys. A*, **122**(7), 673. http://doi.org/10.1007/s00339-016-0196-3.

Ghadiri, M., Shafiei, N. and Alireza MoU.S.A.vi, S. (2016c), "Vibration analysis of a rotating functionally graded tapered microbeam based on the modified couple stress theory by DQEM", *Appl. Phys. A*, **122**(9), 837. http://doi.org/10.1007/s00339-016-0364-5.

Ghadiri, M., Shafiei, N., Salekdeh, S.H., Mottaghi, P. and Mirzaie, T. (2016d), "Investigation of the dental implant geometry effect on stress distribution at dental implant–bone interface", *J. Brazil. Soc. Mech. Sci. Eng.*, **38**(2), 335-343. http://doi.org/10.1007/s40430-015-0472-8.

Ghadiri, M., Mahinzare, M., Shafiei, N. and Ghorbani, K. (2017a), "On size-dependent thermal buckling and free vibration of circular FG Microplates in thermal environments", *Microsyst. Technol.*, **23**(10), 4989-5001. http://doi.org/10.1007/s00542-017-3308-x.

Ghadiri, M., Shafiei, N. and Alavi, H. (2017b), "Thermo-mechanical vibration of orthotropic cantilever and propped cantilever nanoplate using generalized differential quadrature method", *Mech. Adv. Mater. Struct.*, **24**(8), 636-646. http://doi.org/10.1080/15376494.2016.1196770.

Ghadiri, M., Shafiei, N. and Alavi, H. (2017c), "Vibration analysis of a rotating nanoplate using nonlocal elasticity theory", *J. Solid Mech.*, **9**(2), 319-337.

Ghadiri, M., Shafiei, N. and Babaei, R. (2017d), "Vibration of a rotary FG plate with consideration of thermal and Coriolis effects", *Steel Compos. Struct.*, **25**(2), 197-207. http://doi.org/10.12989/SCS.2017.25.2.197.

Ghadiri, M., Shafiei, N. and Safarpour, H. (2017e), "Influence of surface effects on vibration behavior of a rotary functionally graded nanobeam based on Eringen's nonlocal elasticity", *Microsyst. Technol.*, **23**(4), 1045-1065. http://doi.org/10.1007/s00542-016-2822-6.

Ghazanfari, A., Assempour, A., Habibi, M. and Hashemi, R. (2016), "Investigation on the effective range of the through thickness shear stress on forming limit diagram using a modified Marciniak–Kuczynski model", *Modares Mech. Eng.*, **16**(1), 137-143.

Ghazanfari, A., Soleimani, S.S., Keshavarzzadeh, M., Habibi, M., Assempuor, A. and Hashemi, R. (2020), "Prediction of FLD for sheet metal by considering through-thickness shear stresses", *Mech. Based Des. Struct.*, **48**(6), 755-772. http://doi.org/10.1080/15397734.2019.1662310.

Goldring, M.B. and Goldring, S.R. (2010), "Articular cartilage and subchondral bone in the pathogenesis of osteoarthritis", *Ann NY Acad. Sci.* **1192** 230-237. http://doi.org/10.1111/j.1749-6632.2009.05240.x.

Guo, J., Baharvand, A., Tazeddinova, D., Habibi, M., Safarpour, H., Roco-Videla, A. and Selmi, A. (2021), "An intelligent computer method for vibration responses of the spinning multi-layer symmetric nanosystem using multi-physics modeling", *Eng. Comput.*, 1-22. http://doi.org/10.1007/s00366-021-01433-4.

Habibi, M., Hashemi, R., Ghazanfari, A., Naghdabadi, R. and Assempour, A. (2016), "Forming limit diagrams by including the M–K model in finite element simulation considering the effect of bending", *Proceedings of the Institution of Mechanical Engineers, Part L: Journal of Materials: Design and Applications*. **232**(8), 625-636. http://doi.org/10.1177/1464420716642258.

Habibi, M., Hashemi, R., Fallah Tafti, M. and Assempour, A. (2018), "Experimental investigation of mechanical properties, formability and forming limit diagrams for tailor-welded blanks produced by friction stir welding", *J. Manuf. Proc.*, **31**, 310-323. https://doi.org/10.1016/j.jmapro.2017.11.009.

Hadji, L. and Avcar, M. (2021), "Nonlocal free vibration analysis of porous FG nanobeams using hyperbolic shear deformation beam theory", *Adv. Nano Res.*, **10**(3), 281-293. http://doi.org/10.12989/ANR.2021.10.3.281.

Hamidi, A., Houari, M.S.A., Mahmoud, S. and Tounsi, A. (2015), "A sinusoidal plate theory with 5-unknowns and stretching effect for thermomechanical bending of functionally graded sandwich plates", *Steel Compos. Struct.*, **18**(1), 235-253. https://doi.org/10.12989/scs.2015.18.1.235.

Hashemi, H.R., Alizadeh, A.a., Oyarhossein, M.A., Shavalipour, A., Makkiabadi, M. and Habibi, M. (2021), "Influence of imperfection on amplitude and resonance frequency of a reinforcement compositionally graded nanostructure", *Wave. Random Complex Med.*, **31**(6), 1340-1366. http://doi.org/10.1080/17455030.2019.1662968.

Hay *et al*. (2017), "Global, regional, and national disability-adjusted life-years (DALYs) for 333 diseases and injuries and healthy life expectancy (HALE) for 195 countries and territories, 1990-2016: A systematic analysis for the global burden of disease study 2016", *The Lancet*, **390**(10100), 1260-1344. https://doi.org/10.1016/S0140-6736(17)32130-X.

He, X., Ding, J., Habibi, M., Safarpour, H. and Safarpour, M. (2021), "Non-polynomial framework for bending responses of the multi-scale hybrid laminated nanocomposite reinforced circular/annular plate", *Thin Wall. Struct.*, **166**, 108019. https://doi.org/10.1016/j.tws.2021.108019.

Hosseini, S.M.R., Habibi, M. and Assempour, A. (2018), "Experimental and numerical determination of forming limit diagram of steel-copper two-layer sheet considering the interface between the layers", *Modares Mech. Eng.*, **18**(6), 174-181.

Hou, F., Wu, S., Moradi, Z. and Shafiei, N. (2021), "The computational modeling for the static analysis of axially functionally graded micro-cylindrical imperfect beam applying the computer simulation", *Eng. Comput.*, 1-29. https://doi.org/10.1007/s00366-021-01456-x.

Hsu, Y.H. and Kiel, D.P. (2012), "Clinical review: Genome-wide association studies of skeletal phenotypes: What we have learned and where we are headed", *J. Clin Endocrin. Metab.*, **97**(10), E1958-1977. https://doi.org/10.1210/jc.2012-1890.

Hu, J., Zhang, H., Li, Z., Zhao, C., Xu, Z. and Pan, Q. (2021),

"Object traversing by monocular UAV in outdoor environment", *Asian J. Control*, **23**(6), 2766-2775. https://doi.org/10.1002/asjc.2415.

Huang, K. and Sun, B. (2020), "Design of port communication signal management system based on ZigBee", *J. Coastal Res.*, **103**(SI), 735-738. https://doi.org/10.2112/SI103-151.1.

Huang, X., Hao, H., Oslub, K., Habibi, M. and Tounsi, A. (2021a), "Dynamic stability/instability simulation of the rotary size-dependent functionally graded microsystem", *Eng. Comput.*, 1-17. https://doi.org/10.1007/s00366-021-01399-3.

Huang, X., Zhang, Y., Moradi, Z. and Shafiei, N. (2021b), "Computer simulation via a couple of homotopy perturbation methods and the generalized differential quadrature method for nonlinear vibration of functionally graded non-uniform micro-tube", *Eng. Comput.*, 1-18. https://doi.org/10.1007/s00366-021-01395-7.

Huang, X., Zhu, Y., Vafaei, P., Moradi, Z. and Davoudi, M. (2021c), "An iterative simulation algorithm for large oscillation of the applicable 2D-electrical system on a complex nonlinear substrate", *Eng. Comput.*, 1-13. https://doi.org/10.1007/s00366-021-01320-y.

Hung, C.C., Chaya, A., Liu, K., Verdelis, K. and Sfeir, C. (2019), "The role of magnesium ions in bone regeneration involves the canonical Wnt signaling pathway", *Acta Biomater.*, **98**, 246-255. https://doi.org/10.1016/j.actbio.2019.06.001.

Huo, J., Zhang, G., Ghabussi, A. and Habibi, M. (2021), "Bending analysis of FG-GPLRC axisymmetric circular/annular sector plates by considering elastic foundation and horizontal friction force using 3D-poroelasticity theory", *Compos. Struct.*, **276**, 114438. https://doi.org/10.1016/j.compstruct.2021.114438.

Hussain, M., Naeem Muhammad, N., Tounsi, A. and Taj, M. (2019), "Nonlocal effect on the vibration of armchair and zigzag SWCNTs with bending rigidity", *Adv. Nano Res.*, **7**(6), 431-442. https://doi.org/10.12989/ANR.2019.7.6.431.

Hussain, M., Naeem Muhammad, N., Taj, M. and Tounsi, A. (2020), "Simulating vibration of single-walled carbon nanotube using Rayleigh-Ritz's method", *Adv. Nano Res.*, **8**(3), 215-228. https://doi.org/10.12989/ANR.2020.8.3.215.

Islam Molla, M., Furukawa, M., Tateishi, I., Katsumata, H., Suzuki, T., Kaneco, S.J.W.C. and Management (2018), "Photocatalytic degradation of fenitrothion in water with TiO_2 under solar irradiation", *Water Conserv. Manage.*, **2**(2), 1-5. https://doi.org/10.26480/wcm.02.2018.01.05.

Jacobs, J.J., Hallab, N.J., Skipor, A.K. and Urban, R.M. (2003), "Metal degradation products: a cause for concern in metal-metal bearings?", *Clin. Orthop. Relat. R.*, **417**, 139-147. https://doi.org/10.1097/01.blo.0000096810.78689.62.

Jiao, J., Ghoreishi, S.-m., Moradi, Z. and Oslub, K. (2021), "Coupled particle swarm optimization method with genetic algorithm for the static–dynamic performance of the magneto-electro-elastic nanosystem", *Eng. Comput.*, 1-15. https://doi.org/10.1007/s00366-021-01391-x.

Kannan, M.B. and Raman, R.K. (2008), "In vitro degradation and mechanical integrity of calcium-containing magnesium alloys in modified-simulated body fluid", *Biomaterials*, **29**(15), 2306-2314. https://doi.org/10.1016/j.biomaterials.2008.02.003.

Kassahun, G.B. (2019), "High tunability of size dependent optical properties of ZnO@ M@ Au (M= SiO_2, In_2O_3, TiO_2) core/ spacer/shell nanostructure", *Adv. Nano Res.*, **2**(1), 1-13. https://doi.org/10.21467/anr.2.1.1-13.

Kong, X., Wang, L., Li, G., Qu, X., Niu, J., Tang, T., Dai, K., Yuan, G. and Hao, Y. (2018), "Mg-based bone implants show promising osteoinductivity and controllable degradation: A long-term study in a goat femoral condyle fracture model", *Mater. Sci. Eng. C*, **86**, 42-47. https://doi.org/10.1016/j.msec.2017.12.014.

Kosy, J.D., Schranz, P.J., Toms, A.D., Eyres, K.S. and Mandalia, V.I. (2011), "The use of radiofrequency energy for arthroscopic chondroplasty in the knee", *Arthroscopy J. Arthroscopic Relat. Surg.*, **27**(5), 695-703. https://doi.org/10.1016/j.arthro.2010.11.058.

Kreuz, P.C., Steinwachs, M.R., Erggelet, C., Krause, S.J., Konrad, G., Uhl, M. and Südkamp, N. (2006), "Results after microfracture of full-thickness chondral defects in different compartments in the knee", *Osteoarthr. Cartilage*, **14**(11), 1119-1125. https://doi.org/10.1016/j.joca.2006.05.003.

Kwon, H., Brown, W.E., Lee, C.A., Wang, D., Paschos, N., Hu, J.C. and Athanasiou, K.A. (2019), "Surgical and tissue engineering strategies for articular cartilage and meniscus repair", *Nat. Rev. Rheumatol.*, **15**(9), 550-570. https://doi.org/10.1038/s41584-019-0255-1.

Li, G., Yin, J., Gao, J., Cheng, T.S., Pavlos, N.J., Zhang, C. and Zheng, M.H. (2013), "Subchondral bone in osteoarthritis: Insight into risk factors and microstructural changes", *Arthritis. Res. Ther.*, **15**(6), 223. https://doi.org/10.1186/ar4405.

Li, T., Cheng, H., Yuan, H., Xu, Q., Shu, C., Zhang, Y., Xu, P., Tan, J., Rui, Y., Li, P. and Tan, X. (2016), "Antitumor activity of cGAMP via stimulation of cGAS-cGAMP-STING-IRF3 mediated innate immune response", *Sci. Rep.*, **6**, 19049. https://doi.org/10.1038/srep19049.

Li, J., Tang, F. and Habibi, M. (2020a), "Bi-directional thermal buckling and resonance frequency characteristics of a GNP-reinforced composite nanostructure", *Eng. Comput.*, 1-22. https://doi.org/10.1007/s00366-020-01110-y.

Li, Y., Li, S., Guo, K., Fang, X. and Habibi, M. (2020b), "On the modeling of bending responses of graphene-reinforced higher order annular plate via two-dimensional continuum mechanics approach", *Eng. Comput.*, 1-22. https://doi.org/10.1007/s00366-020-01166-w.

Li, X., Yu, Q., Chen, X. and Zhang, Q. (2021), "Microstructures and electrochemical behaviors of casting magnesium alloys with enhanced compression strengths and decomposition rates", *J. Magn. Alloy*, In Press. https://doi.org/10.1016/j.jma.2021.07.018.

Liao, Y., Xu, Q., Zhang, J., Niu, J., Yuan, G., Jiang, Y., He, Y. and Wang, X. (2015), "Cellular response of chondrocytes to magnesium alloys for orthopedic applications", *Int. J. Mol. Med.*, **36**(1), 73-82. https://doi.org/10.3892/ijmm.2015.2211.

Liu, Z., Su, S., Xi, D. and Habibi, M. (2020a), "Vibrational responses of a MHC viscoelastic thick annular plate in thermal environment using GDQ method", *Mech. Based Des. Struct.*, 1-26. https://doi.org/10.1080/15397734.2020.1784201.

Liu, Z., Wu, X., Yu, M. and Habibi, M. (2020b), "Large-amplitude dynamical behavior of multilayer graphene platelets reinforced nanocomposite annular plate under thermo-mechanical loadings", *Mech. Based Des. Struct.*, 1-25. https://doi.org/10.1080/15397734.2020.1815544.

Liu, H., Shen, S., Oslub, K., Habibi, M. and Safarpour, H. (2021a), "Amplitude motion and frequency simulation of a composite viscoelastic microsystem within modified couple stress elasticity", *Eng. Comput.*, 1-15. https://doi.org/10.1007/s00366-021-01316-8.

Liu, H., Zhao, Y., Pishbin, M., Habibi, M., Bashir, M.O. and Issakhov, A. (2021b), "A comprehensive mathematical simulation of the composite size-dependent rotary 3D microsystem via two-dimensional generalized differential quadrature method", *Eng. Comput.*, 1-16. https://doi.org/10.1007/s00366-021-01419-2.

Liu, L., Zhang, X., Zhu, Q., Li, K., Lu, Y., Zhou, X. and Guo, T. (2021c), "Ultrasensitive detection of endocrine disruptors via superfine plasmonic spectral combs", *Light Sci. Appl.*, **10**(1), 1-14. https://doi.org/10.1038/s41377-021-00618-2.

Liu, Y., Wang, W., He, T., Moradi, Z. and Larco Benítez, M.A.

(2021d), "On the modelling of the vibration behaviors via discrete singular convolution method for a high-order sector annular system", *Eng. Comput.*, 1-23. https://doi.org/10.1007/s00366-021-01454-z.

Livak, K.J. and Schmittgen, T.D. (2001), "Analysis of relative gene expression data using real-time quantitative PCR and the 2(-Delta Delta C(T)) Method", *Methods.* **25**(4), 402-408. https://doi.org/10.1006/meth.2001.1262.

Lozano, R.M., Pérez-Maceda, B.T., Carboneras, M., Onofre-Bustamante, E., García-Alonso, M.C. and Escudero, M.L. (2013), "Response of MC3T3-E1 osteoblasts, L929 fibroblasts, and J774 macrophages to fluoride surface-modified AZ31 magnesium alloy", *J Biomed Mater Res A.* **101**(10), 2753-2762. https://doi.org/10.1002/jbm.a.34579.

Lv, B.J., Wang, S., Xu, T.-W. and Guo, F. (2021), "Effects of minor Nd and Er additions on the precipitation evolution and dynamic recrystallization behavior of Mg–6.0Zn–0.5Mn alloy", *J. Magn. Alloys*, **9**(3), 840-852. https://doi.org/10.1016/j.jma.2020.06.018.

Ma, L., Liu, X. and Moradi, Z. (2021), "On the chaotic behavior of graphene-reinforced annular systems under harmonic excitation", *Eng. Comput.*, 1-25. https://doi.org/10.1007/s00366-020-01210-9.

Mao, L., Yuan, G., Niu, J., Zong, Y. and Ding, W. (2013), "In vitro degradation behavior and biocompatibility of Mg-Nd-Zn-Zr alloy by hydrofluoric acid treatment", *Mater. Sci. Eng. C.*, **33**(1), 242-250. https://doi.org/10.1016/j.msec.2012.08.036.

Marcacci, M., Filardo, G. and Kon, E. (2013), "Treatment of cartilage lesions: What works and why?", *Injury*, **44**, S11-S15. https://doi.org/10.1016/S0020-1383(13)70004-4.

Matouk, H., BoU.S.A.hla, A.A., Heireche, H., Bourada, F., Bedia, E., Tounsi, A., Mahmoud, S., Tounsi, A. and Benrahou, K. (2020a), "Investigation on hygro-thermal vibration of P-FG and symmetric S-FG nanobeam using integral Timoshenko beam theory", *Adv. Nano Res.*, **8**(4), 293-305. https://doi.org/10.12989/anr.2020.8.4.293.

Matouk, H., BoU.S.A.hla Abdelmoumen, A., Heireche, H., Bourada, F., Bedia, E.A.A., Tounsi, A., Mahmoud, S.R., Tounsi, A. and Benrahou, K.H. (2020b), "Investigation on hygro-thermal vibration of P-FG and symmetric S-FG nanobeam using integral Timoshenko beam theory", *Adv. Nano Res.*, **8**(4), 293-305. https://doi.org/10.12989/ANR.2020.8.4.293.

Mehar, K. and Panda, S.K. (2019), "Multiscale modeling approach for thermal buckling analysis of nanocomposite curved structure", *Adv. Nano Res.*, **7**(3), 181-190. https://doi.org/10.12989/anr.2019.7.3.181.

Ming, L., Zhipeng, Y., Fei, Y., Feng, R., Jian, W., Baoguo, J., Yongqiang, W. and Peixun, Z. (2018), "Microfluidic-based screening of resveratrol and drug-loading PLA/Gelatine nano-scaffold for the repair of cartilage defect", *Artif. Cells Nanomed. Biotechnol.*, **46**(sup1), 336-346. https://doi.org/10.1080/21691401.2017.1423498.

Mirjavadi, S.S., Afshari, B.M., Shafiei, N., Hamouda, A., Kazemi, M. and Structures, C. (2017a), "Thermal vibration of two-dimensional functionally graded (2D-FG) porous Timoshenko nanobeams", *Steel Compos. Struct.*, **25**(4), 415-426. https://doi.org/10.12989/scs.2017.25.4.415.

Mirjavadi, S.S., Matin, A., Shafiei, N., Rabby, S. and Mohasel Afshari, B. (2017b), "Thermal buckling behavior of two-dimensional imperfect functionally graded microscale-tapered porous beam", *J. Therm. Stresses*, **40**(10), 1201-1214. https://doi.org/10.1080/01495739.2017.1332962.

Mirjavadi, S.S., Mohasel Afshari, B., Shafiei, N., Rabby, S. and Kazemi, M. (2017c), "Effect of temperature and porosity on the vibration behavior of two-dimensional functionally graded micro-scale Timoshenko beam", *J. Vib. Control*, **24**(18), 4211-4225. https://doi.org/10.1177/1077546317721871.

Mirjavadi, S.S., Rabby, S., Shafiei, N., Afshari, B.M. and Kazemi, M. (2017d), "On size-dependent free vibration and thermal buckling of axially functionally graded nanobeams in thermal environment", *Appl. Phys. A*, **123**(5), 315. https://doi.org/10.1007/s00339-017-0918-1.

Moayedi, H., Aliakbarlou, H., Jebeli, M., Noormohammadiarani, O., Habibi, M., Safarpour, H. and Foong, L.K. (2020a), "Thermal buckling responses of a graphene reinforced composite micropanel structure", **12**(01), 2050010. https://doi.org/10.1142/s1758825120500106.

Moayedi, H., Darabi, R., Ghabussi, A., Habibi, M. and Foong, L.K. (2020b), "Weld orientation effects on the formability of tailor welded thin steel sheets", *Thin Wall. Struct.*, **149**, 106669. https://doi.org/10.1016/j.tws.2020.106669.

Moayedi, H., Ebrahimi, F., Habibi, M., Safarpour, H. and Foong, L.K. (2020c), "Application of nonlocal strain–stress gradient theory and GDQEM for thermo-vibration responses of a laminated composite nanoshell", *Eng. Comput.*, **37**(4), 3359-3374. https://doi.org/10.1007/s00366-020-01002-1.

Moradi, Z., Davoudi, M., Ebrahimi, F. and Ehyaei, A.F. (2021), "Intelligent wave dispersion control of an inhomogeneous micro-shell using a proportional-derivative smart controller", *Wave. Random Complex Med.*, 1-24. https://doi.org/10.1080/17455030.2021.1926572.

Najaafi, N., Jamali, M., Habibi, M., Sadeghi, S., Jung, D.w. and Nabipour, N. (2021), "Dynamic instability responses of the substructure living biological cells in the cytoplasm environment using stress-strain size-dependent theory", *J. Biomol. Struct. Dyn.*, **39**(7), 2543-2554. https://doi.org/10.1080/07391102.2020.1751297.

Navi, B.R., Mohammadimehr, M. and Arani, A.G. (2019), "Active control of three-phase CNT/resin/fiber piezoelectric polymeric nanocomposite porous sandwich microbeam based on sinusoidal shear deformation theory", *Steel Compos. Struct.*, **32**(6), 753-767. https://doi.org/10.12989/scs.2019.32.6.753.

Oyarhossein, M.A., Alizadeh, A.a., Habibi, M., Makkiabadi, M., Daman, M., Safarpour, H. and Jung, D.W. (2020), "Dynamic response of the nonlocal strain-stress gradient in laminated polymer composites microtubes", *Sci. Rep.*, **10**(1), 5616. https://doi.org/10.1038/s41598-020-61855-w.

Park, K.S., Kim, B.J., Lih, E., Park, W., Lee, S.H., Joung, Y.K. and Han, D.K. (2018), "Versatile effects of magnesium hydroxide nanoparticles in PLGA scaffold-mediated chondrogenesis", *Acta Biomater.*, **73**, 204-216. https://doi.org/10.1016/j.actbio.2018.04.022.

Pei, Y., Brun, S.N., Markant, S.L., Lento, W., Gibson, P., Taketo, M.M., Giovannini, M., Gilbertson, R.J. and Wechsler-Reya, R.J. (2012), "WNT signaling increases proliferation and impairs differentiation of stem cells in the developing cerebellum", *Development*, **139**(10), 1724-1733. https://doi.org/10.1242/dev.050104.

Peng, D., Chen, S., Darabi, R., Ghabussi, A. and Habibi, M. (2021), "Prediction of the bending and out-of-plane loading effects on formability response of the steel sheets", *Arch. Civil Mech. Eng.*, **21**(2), 74. https://doi.org/10.1007/s43452-021-00227-1.

Puleo, D.A. and Huh, W.W. (1995), "Acute toxicity of metal ions in cultures of osteogenic cells derived from bone marrow stromal cells", *J. Appl. Biomater.*, **6**(2), 109-116. https://doi.org/10.1002/jab.770060205.

Samsa, W.E., Vasanji, A., Midura, R.J. and Kondratov, R.V. (2016), "Deficiency of circadian clock protein BMAL1 in mice results in a low bone mass phenotype", *Bone*, **84**, 194-203. https://doi.org/10.1016/j.bone.2016.01.006.

Semmah, A., Heireche, H., BoU.S.A.hla, A.A. and Tounsi, A. (2019), "Thermal buckling analysis of SWBNNT on Winkler foundation by non local FSDT", *Adv. Nano Res.*, **7**(2), 89-98.

https://doi.org/10.12989/anr.2019.7.2.089.
Shafiei, N., Kazemi, M. and Ghadiri, M. (2016a), "Comparison of modeling of the rotating tapered axially functionally graded Timoshenko and Euler–Bernoulli microbeams", *Physica E.*, **83**, 74-87. https://doi.org/10.1016/j.physe.2016.04.011.
Shafiei, N., Kazemi, M. and Ghadiri, M. (2016b), "Nonlinear vibration behavior of a rotating nanobeam under thermal stress using Eringen's nonlocal elasticity and DQM", *Appl. Phys. A*, **122**(8), 728. https://doi.org/10.1007/s00339-016-0245-y.
Shafiei, N., Kazemi, M. and Ghadiri, M. (2016c), "Nonlinear vibration of axially functionally graded tapered microbeams", *Int. J. Eng. Sci.*, **102**, 12-26. https://doi.org/10.1016/j.ijengsci.2016.02.007.
Shafiei, N., Kazemi, M. and Ghadiri, M. (2016d), "On size-dependent vibration of rotary axially functionally graded microbeam", *Int. J. Eng. Sci.*, **101**, 29-44. https://doi.org/10.1016/j.ijengsci.2015.12.008.
Shafiei, N., Kazemi, M., Safi, M. and Ghadiri, M. (2016e), "Nonlinear vibration of axially functionally graded non-uniform nanobeams", *Int. J. Eng. Sci.*, **106**, 77-94. https://doi.org/10.1016/j.ijengsci.2016.05.009.
Shafiei, N., MoU.S.A.vi, A. and Ghadiri, M. (2016f), "On size-dependent nonlinear vibration of porous and imperfect functionally graded tapered microbeams", *Int. J. Eng. Sci.*, **106**, 42-56. https://doi.org/10.1016/j.ijengsci.2016.05.007.
Shafiei, N., MoU.S.A.vi, A. and Ghadiri, M. (2016g), "Vibration behavior of a rotating non-uniform FG microbeam based on the modified couple stress theory and GDQEM", *Compos. Struct.*, **149** 157-169. https://doi.org/10.1016/j.compstruct.2016.04.024.
Shafiei, N. and Kazemi, M. (2017a), "Buckling analysis on the bi-dimensional functionally graded porous tapered nano-/micro-scale beams", *Aerosp. Sci. Technol.*, **66**, 1-11. https://doi.org/10.1016/j.ast.2017.02.019.
Shafiei, N. and Kazemi, M. (2017b), "Nonlinear buckling of functionally graded nano-/micro-scaled porous beams", *Compos. Struct.*, **178**, 483-492. https://doi.org/10.1016/j.compstruct.2017.07.045.
Shafiei, N., Ghadiri, M., Makvandi, H. and Hosseini, S.A. (2017a), "Vibration analysis of Nano-Rotor's Blade applying Eringen nonlocal elasticity and generalized differential quadrature method", *Appl. Math. Modell.*, **43**, 191-206. https://doi.org/10.1016/j.apm.2016.10.061.
Shafiei, N., Kazemi, M. and Fatahi, L. (2017b), "Transverse vibration of rotary tapered microbeam based on modified couple stress theory and generalized differential quadrature element method", *Mech. Adv. Mater. Struct.*, **24**(3), 240-252. https://doi.org/10.1080/15376494.2015.1128025.
Shafiei, N., Mirjavadi, S.S., Afshari, B.M., Rabby, S. and Hamouda, A.M.S. (2017c), "Nonlinear thermal buckling of axially functionally graded micro and nanobeams", *Compos. Struct.*, **168**, 428-439. https://doi.org/10.1016/j.compstruct.2017.02.048.
Shafiei, N., Mirjavadi, S.S., MohaselAfshari, B., Rabby, S. and Kazemi, M. (2017d), "Vibration of two-dimensional imperfect functionally graded (2D-FG) porous nano-/micro-beams", *Comput. Method Appl. M.*, **322**, 615-632. https://doi.org/10.1016/j.cma.2017.05.007.
Shafiei, N. and She, G.L. (2018), "On vibration of functionally graded nano-tubes in the thermal environment", *Int. J. Eng. Sci.*, **133**, 84-98. https://doi.org/10.1016/j.ijengsci.2018.08.004.
Shafiei, N., Ghadiri, M. and Mahinzare, M. (2019), "Flapwise bending vibration analysis of rotary tapered functionally graded nanobeam in thermal environment", *Mech. Adv. Mater. Struct.*, **26**(2), 139-155. 10.1080/15376494.2017.1365982.
Shafiei, N., Hamisi, M. and Ghadiri, M. (2020), "Vibration analysis of rotary tapered axially functionally graded Timoshenko nanobeam in thermal environment", *J. Solid Mech.*, **12**(1), 16-32.
Shao, Y., Zhao, Y., Gao, J. and Habibi, M. (2021), "Energy absorption of the strengthened viscoelastic multi-curved composite panel under friction force", *Arch. Civil Mech. Eng.*, **21**(4), 141. https://doi.org/10.1007/s43452-021-00279-3.
Shariati, A., Habibi, M., Tounsi, A., Safarpour, H. and Safa, M. (2021), "Application of exact continuum size-dependent theory for stability and frequency analysis of a curved cantilevered microtubule by considering viscoelastic properties", *Eng. Comput.*, **37**(4), 3629-3648. https://doi.org/10.1007/s00366-020-01024-9.
Shariati, A., Jung, D.W., Mohammad-Sedighi, H., Żur, K.K., Habibi, M. and Safa, M. (2020a), "On the vibrations and stability of moving viscoelastic axially functionally graded nanobeams", *Materials*, **13**(7), 1707. https://doi.org/10.3390/ma13071707.
Shariati, A., Jung, D.W., Mohammad-Sedighi, H., Żur, K.K., Habibi, M. and Safa, M. (2020b), "Stability and dynamics of viscoelastic moving rayleigh beams with an asymmetrical distribution of material parameters", *Symmetry*, **12**(4), 586. https://doi.org/10.3390/sym12040586.
Shi, X., Li, J. and Habibi, M. (2020), "On the statics and dynamics of an electro-thermo-mechanically porous GPLRC nanoshell conveying fluid flow", *Mech. Based Des. Struct.*, 1-37. https://doi.org/10.1080/15397734.2020.1772088.
Shivanian, E., Ghadiri, M. and Shafiei, N. (2017), "Influence of size effect on flapwise vibration behavior of rotary microbeam and its analysis through spectral meshless radial point interpolation", *Appl. Phys. A*, **123**(5), 329. https://doi.org/10.1007/s00339-017-0955-9.
Tounsi, A., Benguediab, S., Semmah, A. and Zidour, M.J.A.i.n.r. (2013), "Nonlocal effects on thermal buckling properties of double-walled carbon nanotubes", *Adv. Nano Res.*, **1**(1), 1-11. https://doi.org/10.12989/anr.2013.1.1.001.
Wang, W., Jia, G., Wang, Q., Huang, H., Li, X., Zeng, H., Ding, W., Witte, F., Zhang, C., Jia, W. and Yuan, G. (2020a), "The in vitro and in vivo biological effects and osteogenic activity of novel biodegradable porous Mg alloy scaffolds", *Mater. Des.*, **189**, 108514. https://doi.org/10.1016/j.matdes.2020.108514.
Wang, Y., Ouyang, Y., Pang, X., Mao, L., Yuan, G., Jiang, Y. and He, Y. (2012), "Effects of degradable MG-ND-ZN-ZR alloy on osteoblastic cell function", *Int. J. Immunopath. Ph.*, **25**(3), 597-606. https://doi.org/10.1177/039463201202500306.
Wang, Z., Yu, S., Xiao, Z. and Habibi, M. (2020b), "Frequency and buckling responses of a high-speed rotating fiber metal laminated cantilevered microdisk", *Mech. Adv. Mater. Struct.*, 1-14. https://doi.org/10.1080/15376494.2020.1824284.
Witte, F., Kaese, V., Haferkamp, H., Switzer, E., Meyer-Lindenberg, A., Wirth, C.J. and Windhagen, H. (2005), "In vivo corrosion of four magnesium alloys and the associated bone response", *Biomaterials*, **26**(17), 3557-3563. https://doi.org/10.1016/j.biomaterials.2004.09.049.
Wu, J. and Habibi, M. (2021), "Dynamic simulation of the ultra-fast-rotating sandwich cantilever disk via finite element and semi-numerical methods", *Eng. Comput.*, 1-17. https://doi.org/10.1007/s00366-021-01396-6.
Xu, W., Pan, G., Moradi, Z. and Shafiei, N. (2021), "Nonlinear forced vibration analysis of functionally graded non-uniform cylindrical microbeams applying the semi-analytical solution", *Compos. Struct.*, **275**, 114395. https://doi.org/10.1016/j.compstruct.2021.114395.
Xu, J., Hu, P., Zhang, X., Chen, J., Wang, J., Zhang, J., Chen, Z., Yu, M.K., Chung, Y.W., Wang, Y., Zhang, X., Zhang, Y., Zheng, N., Yao, H., Yue, J., Chan, H.C., Qin, L. and Ruan, Y.C. (2022), "Magnesium implantation or supplementation ameliorates bone disorder in CFTR-mutant mice through an ATF4-dependent Wnt/β-catenin signaling", *Bioact. Mater.*, **8**, 95-108.

https://doi.org/10.1016/j.bioactmat.2021.06.034.
Yan, Y., Feng, L., Shi, M., Cui, C. and Liu, Y. (2020), "Effect of plasma-activated water on the structure and in vitro digestibility of waxy and normal maize starches during heat-moisture treatment", *Food Chem*., **306**, 125589. https://doi.org/10.1016/j.foodchem.2019.125589.
Yang, J., Sun, H., Xu, D. and Yang, D. (2020), "Separation algorithm of interference signal in anonymous communication of ship wireless network", *J. Coastal Res*., **103**(SI), 896-899. https://doi.org/10.2112/SI103-186.1.
Yang, Y., Sun, F., Chen, H., Tan, H., Yang, L., Zhang, L., Xie, J., Sun, J., Huang, X. and Huang, Y. (2021), "Postnatal exposure to DINP was associated with greater alterations of lipidomic markers for hepatic steatosis than DEHP in postweaning mice", *Sci. Total Environ*., **758**, 143631. https://doi.org/10.1016/j.scitotenv.2020.143631.
Yu, X., Maalla, A. and Moradi, Z. (2022), "Electroelastic high-order computational continuum strategy for critical voltage and frequency of piezoelectric NEMS via modified multi-physical couple stress theory", *Mech. Syst. Signal Pr*., **165**, 108373. https://doi.org/10.1016/j.ymssp.2021.108373.
Zhang, J., Hiromoto, S., Yamazaki, T., Niu, J., Huang, H., Jia, G., Li, H., Ding, W. and Yuan, G. (2016), "Effect of macrophages on in vitro corrosion behavior of magnesium alloy", *J. Biomed. Mater. Res. A*, **104**(10), 2476-2487. https://doi.org/10.1002/jbm.a.35788.
Zhang, L., Chen, Z., Habibi, M., Ghabussi, A. and Alyousef, R. (2021a), "Low-velocity impact, resonance, and frequency responses of FG-GPLRC viscoelastic doubly curved panel", *Compos. Struct.*, **269**, 114000. https://doi.org/10.1016/j.compstruct.2021.114000.
Zhang, X., Shamsodin, M., Wang, H., NoormohammadiArani, O., Khan, A.M., Habibi, M. and Al-Furjan, M.S.H. (2021b), "Dynamic information of the time-dependent tobullian biomolecular structure using a high-accuracy size-dependent theory", *J. Biomol. Struct. Dyn*., **39**(9), 3128-3143. https://doi.org/10.1080/07391102.2020.1760939.
Zhang, X., Yuan, G., Mao, L., Niu, J., Fu, P. and Ding, W. (2012a), "Effects of extrusion and heat treatment on the mechanical properties and biocorrosion behaviors of a Mg-Nd-Zn-Zr alloy", *J. Mech. Behav. Biomed. Mater*., **7**, 77-86. https://doi.org/10.1016/j.jmbbm.2011.05.026.
Zhang, X., Yuan, G., Niu, J., Fu, P. and Ding, W. (2012b), "Microstructure, mechanical properties, biocorrosion behavior, and cytotoxicity of as-extruded Mg-Nd-Zn-Zr alloy with different extrusion ratios", *J. Mech. Behav. Biomed. Mater*., **9**, 153-162. https://doi.org/10.1016/j.jmbbm.2012.02.002.
Zhao, Y., Moradi, Z., Davoudi, M. and Zhuang, J. (2021), "Bending and stress responses of the hybrid axisymmetric system via state-space method and 3D-elasticity theory", *Eng. Comput.*, 1-23. https://doi.org/10.1007/s00366-020-01242-1.
Zhou, C., Zhao, Y., Zhang, J., Fang, Y. and Habibi, M. (2020), "Vibrational characteristics of multi-phase nanocomposite reinforced circular/annular system", *Adv. Nano Res*., **9**(4), 295-307. https://doi.org/10.12989/ANR.2020.9.4.295.
Zhu, M., Chen, M., Zuscik, M., Wu, Q., Wang, Y.J., Rosier, R.N., O'Keefe, R.J. and Chen, D. (2008), "Inhibition of beta-catenin signaling in articular chondrocytes results in articular cartilage destruction", *Arthritis Rheum*., **58**(7), 2053-2064. https://doi.org/10.1002/art.23614.
Zilberman, M. and Eberhart, R.C. (2006), "Drug-eluting bioresorbable stents for various applications", *Annu. Rev. Biomed. Eng*., **8**, 153-180. https://doi.org/10.1146/annurev.bioeng.8.013106.151418.